Weighted Essentially Non-Oscillatory limiters for Runge-Kutta Discontinuous Galerkin Methods

Jianxian Qiu

School of Mathematical Science
Xiamen University

jxqiu@xmu.edu.cn
http://ccam.xmu.edu.cn/teacher/jxqiu

Collaborators: J. Zhu (NUAA), C.-W. Shu (Brown), H. Zhu (NUPT), X. Zhong (MSU), G. Li (Qingdao), Y. Cheng (Baidu Company, Beijing), M. Dumbser (Trento)

Outline

- **Introduction**
- **Numerical Method**
- **Numerical results**
- **Conclusions**

1 Introduction

- We consider hyperbolic conservation laws:

$$\begin{cases} u_t + \nabla \cdot f(u) = 0, \\ u(x,0) = u_0(x). \end{cases}$$

- Hyperbolic conservation laws and convection dominated PDEs play an important role arise in applications, such as gas dynamics, modeling of shallow waters,...

- There are special difficulties associated with solving these systems both on mathematical and numerical methods, for discontinuous may appear in the solutions for nonlinear equations, even though the initial conditions are smooth enough.

Introduction

- This is why devising robust, accurate and efficient methods for numerically solving these problems is of considerable importance and as expected, has attracted the interest of many researchers and practitioners.
- Within recent decades, many high-order numerical methods have been developed to solve these problem. Among them, we would like to mention Discontinuous Galerkin (DG) method and Weighted essentially non-oscillatory (WENO) scheme.
- DG method is a high order finite element method.
- WENO scheme is finite difference or finite volume scheme.
- Both DG and WENO are very important numerical methods for the Convection Dominated PDEs.

Introduction

- The first DG was presented by Reed and Hill in 1973, in the framework of neutron transport (steady state linear hyperbolic equations).
- From 1987, a major development of the DG method was carried out by Cockburn, Shu *et al.* in a series of papers.
- They established a framework to easily solve *nonlinear* time dependent hyperbolic conservation laws using explicit, nonlinearly stable high order Runge-Kutta time discretization and DG discretization in space. These methods are termed RKDG methods.
- DG employs useful features from high resolution finite volume schemes, such as the exact or approximate Riemann solvers serving as numerical fluxes, and limiters.

Introduction

- Limiter is an important component of RKDG methods for solving convection dominated problems with strong shocks in the solutions, which is applied to detect discontinuities and control spurious oscillations near such discontinuities.
- Many such limiters have been used in the literature on RKDG methods such as the minmod type TVB limiter by Coukburn and Shu *et al.*, the moment based limiter developed by Flaherty *et al.*.
- Limiters have been an extensively studied subject for the DG methods, however it is still a challenge to find limiters which are robust, maintaining high order accuracy in smooth regions including at smooth extrema, and yielding sharp, non-oscillatory discontinuity transitions.

WENO schemes have following advantages:

- Uniform high order accuracy in smooth regions including at smooth extrema
- Sharp and essentially non-oscillatory (to the eyes) shock transition.
- Robust for many physical systems with strong shocks.
- Especially suitable for simulating solutions containing both discontinuities and complicated smooth solution structure, such as shock interaction with vortices.
- The limiters used to control spurious oscillations in the presence of strong shocks are less robust than the strategies of WENO finite volume and finite difference methods.
- In this presentation , we would like to show the design of a robust limiter for the RKDG methods based on WENO methods.

2 Numerical Methods

We consider one dimensional conservation laws:

$$u_t + f(u)_x = 0.$$

Let x_i are the centers of the cells $I_i = [x_{i-\frac{1}{2}}, x_{i+\frac{1}{2}}]$, $\Delta x_i = x_{i+\frac{1}{2}} - x_{i-\frac{1}{2}}$, $h = \sup_i \Delta x_i$. The solution and the test function space:

$$V_h^k = \{p : p|_{I_i} \in P^k(I_i)\}.$$

- A local orthogonal basis over I_i,

$$v_0^{(i)}(x) = 1, \qquad v_1^{(i)}(x) = \frac{x - x_i}{\Delta x_i}, \qquad v_2^{(i)}(x) = \left(\frac{x - x_i}{\Delta x_i}\right)^2 - \frac{1}{12}, \cdots$$

Numerical Method

- The numerical solution $u^h(x,t)$:

$$u^h(x,t) = \sum_{l=0}^{k} u_i^{(l)}(t) v_l^{(i)}(x), \qquad \text{for } \; x \in I_i$$

- The degrees of freedom $u_i^{(l)}(t)$ are the moments:

$$u_i^{(l)}(t) = \frac{1}{a_l} \int_{I_i} u^h(x,t) v_l^{(i)}(x) dx, \qquad l = 0, 1, \cdots, k$$

where $a_l = \int_{I_i} (v_l^{(i)}(x))^2 dx$

Numerical Method

- In order to evolve the degrees of freedom $u_i^{(l)}(t)$, we time equation $u_t + f(u)_x = 0$ with basis $v_l^{(i)}(x)$, and integrate it on cell I_i, using integration by part, we obtain:

$$\frac{d}{dt}u_i^{(l)}(t) + \frac{1}{a_l}\Big(-\int_{I_i} f(u^h(x,t))\frac{d}{dx}v_l^{(i)}(x)dx + f(u^h(x_{i+1/2},t))v_l^{(i)}(x_{i+1/2})$$
$$-f(u^h(x_{i-1/2},t))v_l^{(i)}(x_{i-1/2})\Big) = 0, \qquad l = 0, 1, \cdots, k$$

- However, the boundary terms $f(u_{i+1/2})$ and $v_{i+1/2}$ etc. are not well defined when u and v are in this space, as they are discontinuous at the cell interfaces.

Numerical Method

- From the conservation and stability (upwinding) considerations, we take
  - A single valued monotone numerical flux to replace $f(u_{i+1/2})$:

$$\hat{f}_{i+1/2} = \hat{f}(u^-_{i+1/2}, u^+_{i+1/2})$$

  where $\hat{f}(u;u) = f(u)$ (consistency); $\hat{f}(\uparrow,\downarrow)$ (monotonicity) and $\hat{f}$ is Lipschitz continuous with respect to both arguments.
  - Values from inside I_i for the test function v: $v_l^{(i)}(x^-_{i+1/2}),\ v_l^{(i)}(x^+_{i-1/2})$
- We get semi-discretization scheme:

$$\frac{d}{dt}u_i^{(l)}(t) + \frac{1}{a_l}\Big(-\int_{I_i} f(u^h(x,t))\frac{d}{dx}v_l^{(i)}(x)dx + \hat{f}(u^-_{i+1/2}, u^+_{i+1/2})v_l^{(i)}(x^-_{i+1/2})$$
$$-\hat{f}(u^-_{i-1/2}, u^-_{i+1/2})v_l^{(i)}(x^+_{i-1/2})\Big) = 0, \qquad l = 0, 1, \cdots, k. \qquad (*)$$

Numerical Method

Using explicit, nonlinearly stable high order Runge-Kutta time discretizations. [Shu and Osher, JCP, 1988]
The semidiscrete scheme $(*)$ is written as:

$$u_t = L(u)$$

is discretized in time by a nonlinearly stable Runge-Kutta time discretization, e.g. the third order version.

$$\begin{aligned} u^{(1)} &= u^n + \Delta t L(u^n) \\ u^{(2)} &= \frac{3}{4}u^n + \frac{1}{4}u^{(1)} + \frac{1}{4}\Delta t L(u^{(1)}) \\ u^{n+1} &= \frac{1}{3}u^n + \frac{2}{3}u^{(2)} + \frac{2}{3}\Delta t L(u^{(2)}). \end{aligned}$$

Numerical Method

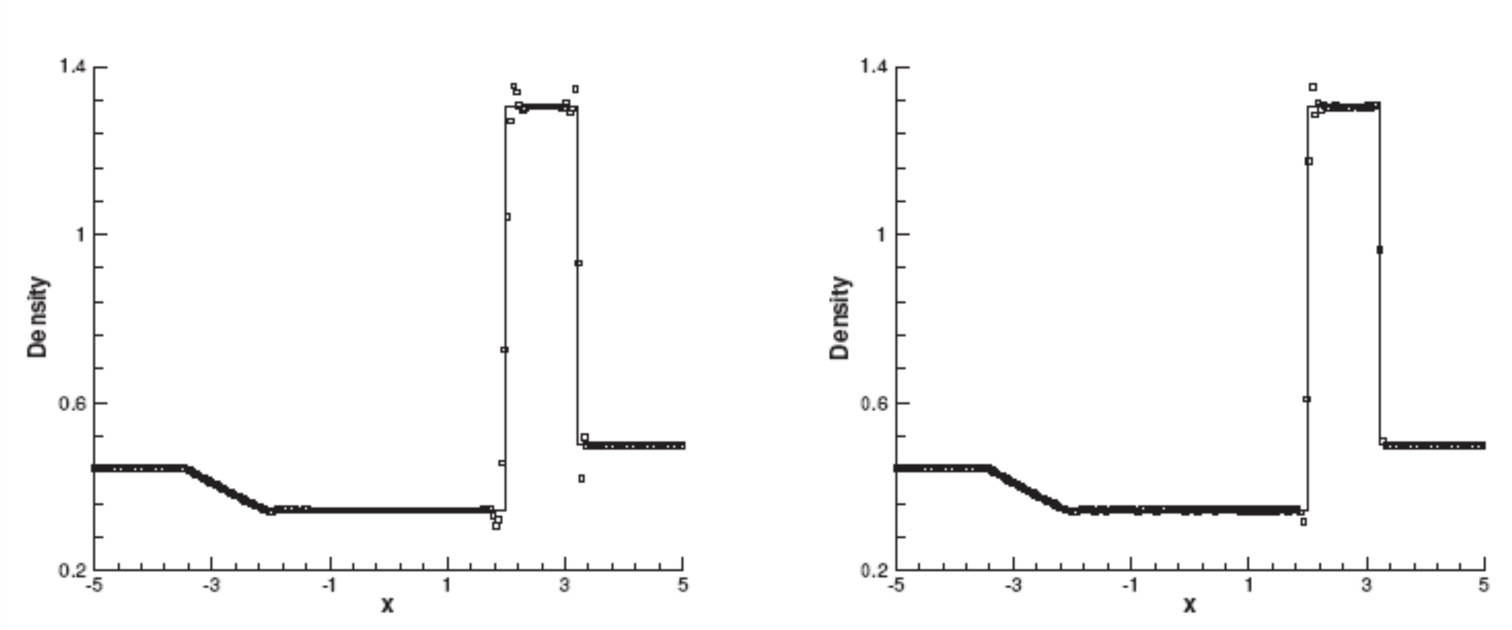

Lax problem. $t = 1.3$. 200 cells. Density. Left: $k = 1$. Right: $k = 2$. $k = 3$ code blows up.

For Blast Wave problem, code blows up for any k.

Limiters

Many limiters have been used in the literature, such as:

- The minmod based TVB limiter.(Cockburn and Shu, Math. Comp. 1989)
- Moment limiter. (Biswas, Devine and Flaherty, Appl. Numer. Math, 1994)
- A modification of moment limiter.(Burbean, Sagaut and Brunean, JCP, 2001)
- The monotonicity preserving (MP) limiter. (Suresh and Huynh, JCP, 1997)
- A modification of the MP limiter. (Rider and Margolin, JCP, 2001)

Numerical Method

These limiters tend to degrade accuracy when mistakenly used in smooth regions of the solution.

	N	L_1 error	L_1 order	L_∞ error	L_∞ order
P^1	10	1.29e-01		3.49e-01	
	20	3.35e-02	1.85	1.13e-01	1.63
	40	8.53e-03	1.97	4.49e-02	1.33
	80	2.16e-03	1.98	1.37e-02	1.71
P^2	10	2.07e-02		1.69e-01	
	20	2.52e-03	3.03	3.01e-02	2.49
	40	4.25e-04	2.57	1.03e-03	1.55
	80	7.56e-05	2.49	3.37e-04	1.61

Burgers equation, initial condition $u(x,0) = \frac{1}{4} + \frac{1}{2}\sin(\pi(2x-10))$, with periodic boundary condition, RKDG with TVB limiter, t=0.05. Cockburn and Shu, JSC (2001)

Nu

Accuracy for 1D Transport Equation, $u_0(x) = sin(\pi x)$

	Δ_x	P^1 (Second order) L^∞-error	Order	P^2 (Third order) L^∞-error	Order	P^3 (Fourth order) L^∞-error	Order
Unlimited	1/16	2.85E-03	—	3.22E-05	—	4.62E-07	—
	1/32	6.81E-04	2.06	4.03E-06	3.00	2.89E-08	3.99
	1/64	1.66E-04	2.03	5.04E-07	3.00	1.81E-09	3.99
	1/128	4.10E-05	2.02	6.29E-08	3.00	1.13E-10	3.99
	1/256	1.02E-05	2.01	7.86E-09	3.00	7.96E-12	3.83
DG^{min}	1/16	3.17E-02	—	8.75E-04	—	1.43E-05	—
	1/32	1.05E-02	1.59	1.64E-04	2.41	1.31E-06	3.44
	1/64	3.47E-03	1.60	2.92E-05	2.49	1.21E-07	3.44
	1/128	1.13E-03	1.61	5.10E-06	2.51	1.10E-08	3.45
	1/256	3.68E-04	1.62	8.88E-07	2.52	1.00E-09	3.46
DG^{max}	1/16	2.75E-02	-	8.01E-04	—	6.31E-06	—
	1/32	1.04E-02	1.39	1.50E-04	2.42	7.91E-07	2.99
	1/64	3.17E-03	1.72	2.74E-05	2.45	9.78E-08	3.01
	1/128	8.97E-04	1.82	4.97E-06	2.46	1.00E-08	3.28
	1/256	2.95E-04	1.60	8.8E-07	2.49	9.59E-10	3.39

Burbean, Sagaut and Brunean, JCP, (2001)

WENO Type limiter

In order to overcome the drawback of these limiters, from 2003, with my colleagues, we have studied using WENO as limiter for RKDG methods, with the goal of obtaining a robust and high order limiting procedure to simultaneously obtain uniform high order accuracy and sharp, non-oscillatory shock transition for RKDG methods.

We separate limiter procedure into two parts:

- Identify the ”troubled cells”, namely those cells which might need the limiting procedure;
- Reconstruct polynomials in ”troubled cells” using WENO reconstruction which only maintain the original cell averages (conservation).

Numerical Method

- For the first part, we can use the following troubled-cell indicators:
  - TVB: based on the TVB minmod function
  - BDF: moment limiter of Biswas, Devine and Flaherty
  - BSB: modified moment limiter of Burbeau *et al.*
  - MP: monotonicity-preserving limiter
  - MMP: modified monotonicity-preserving limiter
  - KXRCF: A shock detector of Krivodonova *et al.* , Applied Numer. Math (2004)
  - Harten: Discontinuous detection technique based on Harten's subcell resolution, (Qiu and Shu, SISC, 2005).

Numerical Method

- TVB indicator

Let $\tilde{u}_i = u^h(x^-_{i+1/2}) - u_i^{(0)}, \qquad \tilde{\tilde{u}}_i = -u^h(x^+_{i-1/2}) + u_i^{(0)}$.
These are modified by the modified minmod function

$$\tilde{u}_i^{(mod)} = \tilde{m}(\tilde{u}_i, u_{i+1}^{(0)} - u_i^{(0)}, u_i^{(0)} - u_{i-1}^{(0)}),$$
$$\tilde{\tilde{u}}_i^{(mod)} = \tilde{m}(\tilde{\tilde{u}}_i, u_{i+1}^{(0)} - u_i^{(0)}, u_i^{(0)} - u_{i-1}^{(0)}),$$

where $\tilde{m}$ is given by

$$\tilde{m}(a_1, a_2, \ldots, a_n) = \begin{cases} a_1 & \text{if } |a_1| \leq M(\Delta x)^2, \\ m(a_1, a_2, \ldots, a_n) & \text{otherwise.} \end{cases}$$

Numerical Method

The minmod function m is given by

$$
\begin{aligned}
& m(a_1, a_2, \ldots, a_n) \\
&= \begin{cases} s \cdot \min_{1 \le j \le n} |a_i| & \text{if } sign(a_1) = \cdots = sign(a_n) = s, \\ 0 & \text{otherwise.} \end{cases}
\end{aligned}
$$

If $\tilde{u}_i^{(mod)} \neq \tilde{u}_i$ or $\tilde{\tilde{u}}_i^{(mod)} \neq \tilde{\tilde{u}}_i$, we declare the cell I_i as a troubled cell.

- KXRCF indicator

Partition the boundary of a cell I_i into two portions ∂I_i^- (inflow, $\overrightarrow{v} \cdot \overrightarrow{n} < 0$) and ∂I_i^+ (outflow, $\overrightarrow{v} \cdot \overrightarrow{n} > 0$). The cell I_i is identified as a troubled cell, if

$$\frac{\left|\int_{\partial I_i^-}(u^h|_{I_i} - u^h|_{I_{n_i}})ds\right|}{h_i^{\frac{k+1}{2}}|\partial I_i^-|||u^h|_{I_i}||} > 1,$$

here h_i is the radius of the circumscribed circle in the element I_i. I_{n_i} is the neighbor of I_i on the side of ∂I_i^- and the norm is based on an element average in one-dimensional case.

- WENO reconstruction

Reconstruct polynomials in "troubled cells" using WENO reconstruction which only maintain the original cell averages (conservation).

$$\begin{tikzcd} \{u_i^{(0)}\} \arrow[rr, "A"] \arrow[dr, "B"'] & & \{u_i^{(l)}, l = 1, \cdots, k\} \\ & \{u(x_G)\} \arrow[ur] & \end{tikzcd}$$

x_G is Gauss or Gauss-Lobatto quadrature point

Numerical M

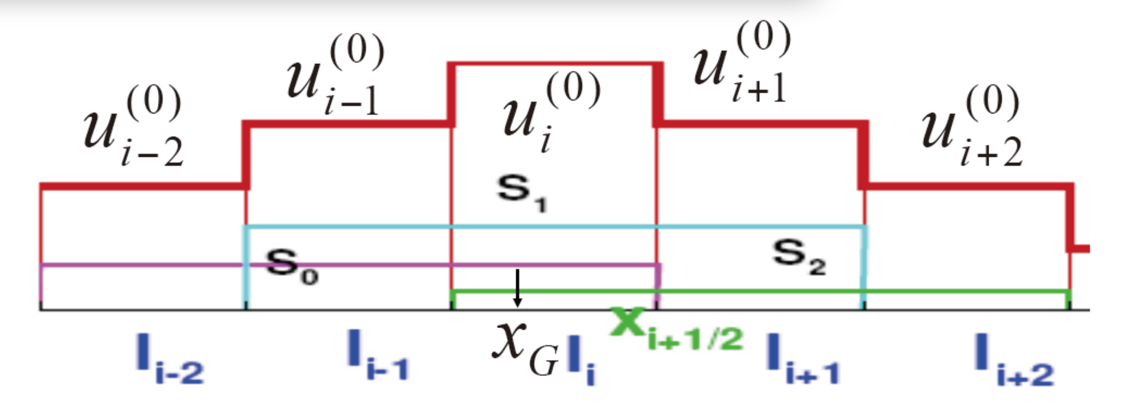

$$S_0: \ \frac{1}{\Delta x}\int_{I_{i+l}} q_0(x)dx = u_{i+l}^{(0)}, \quad l=-k,\cdots,0;$$

$$S_1: \ \frac{1}{\Delta x}\int_{I_{i+l}} q_1(x)dx = u_{i+l}^{(0)}, \quad l=-k+1,\cdots,1;$$

$$\cdots$$

$$S_k: \ \frac{1}{\Delta x}\int_{I_{i+l}} q_k(x)dx = u_{i+l}^{(0)}, \quad l=0,\cdots,k;$$

$$\mathcal{T}: \ \frac{1}{\Delta x}\int_{I_{i+l}} Q(x)dx = u_{i+l}^{(0)}, \quad l=-k,\cdots,k;$$

Numerical Method

- We find the combination coefficients, also called linear weights γ_j, $j = 0, 1, \cdots, k$ satisfying:

$$A: \quad \int_{I_i} Q(x) v_l^{(i)}(x) dx = \sum_{j=0}^{k} \gamma_j \int_{I_i} q_j(x) v_l^{(i)}(x) dx, \quad l = 1, \cdots, k$$

$$B: \quad Q(x_G) = \sum_{j=0}^{k} \gamma_j q_j(x_G).$$

Numerical Method

- We compute the smoothness indicator, denoted as β_j for each stencil S_j, which measures how smooth the function $q_j(x)$ on cell I_i,

$$\beta_j = \sum_{l=1}^{k} \int_{x_{i-1/2}}^{x_{i+1/2}} (\Delta x)^{2l-1} (q_j^{(l)})^2 dx,$$

where $q_j^{(l)}$ is the lth-derivative of $q_j(x)$.

- We compute the nonlinear weight ω_j based on the smoothness indicator

$$\omega_j = \frac{\alpha_j}{\sum_{l=0}^{k} \alpha_l}, \text{ with } \alpha_j = \frac{\gamma_j}{(\varepsilon + \beta_j)^2}, \; j = 0, 1, \ldots, k,$$

where $\varepsilon > 0$ is a small number to avoid the denominator to become 0.

Numerical Method

- The final WENO approximation is then given by:

$$A: \quad u_i^{(l)} = \frac{1}{a_l} \sum_{j=0}^{k} \omega_j \int_{I_i} q_j(x) v_l^{(i)}(x) dx, \quad l = 1, \cdots, k;$$

$$B: \quad u(x_G) = \sum_{j=0}^{k} \omega_j q_j(x_G).$$

- Reconstruction of moments based on the reconstructed point values:

$$u_i^{(l)} = \frac{\Delta x}{a_l} \sum_G w_G u(x_G) v_l^{(i)}(x_G), \quad l = 1, \cdots, k.$$

Remark I:

- For procedure A, there are not the linear weights for $\mathbb{P}^3$ case.

Numerical Method

For procedure B:

- For the $\mathbb{P}^1$ case, we use the two-point Gauss quadrature points.
- For the $\mathbb{P}^2$ case, we use either the four-point Gauss-Lobatto quadrature points or three-point Gauss quadrature points. But there are negative linear weights when three-point Gauss quadrature points are used.
- For the $\mathbb{P}^3$ case, we use the four-point Gauss quadrature points.

Remark II:

WENO limiters work well in all our numerical test cases, including 1D, 2D and 3D, structure and unstructured meshes, but for $\mathbb{P}^2$ and $\mathbb{P}^3$ cases, the compactness of DG is destroyed.

- Hermite WENO (HWENO) reconstruction

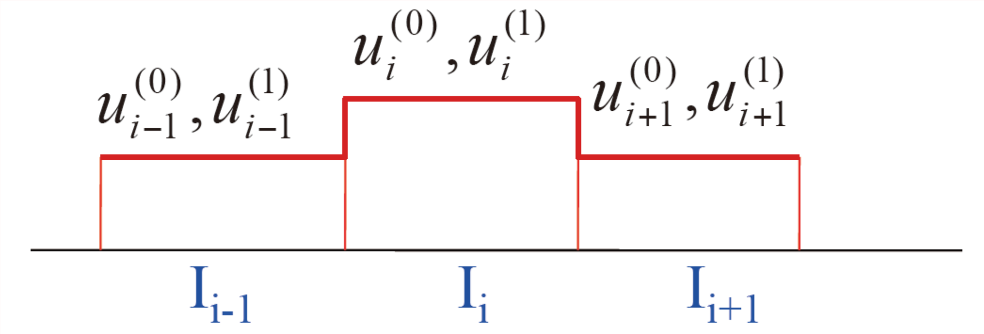

Reconstruct polynomials which maintain the original cell averages (conservation).

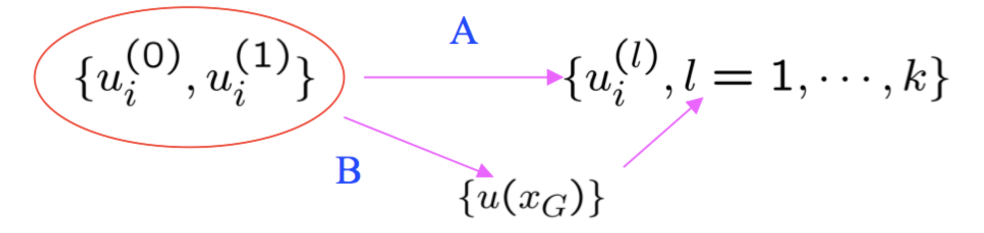

For $\mathbb{P}^2$ case, we obtain following reconstructed polynomials:

$$\int_{I_{i+j}} q_0(x)dx = u_{i+j}^{(0)} a_0, \quad j=-1,0; \qquad \int_{I_{i-1}} q_0(x) v_1^{(i-1)}(x)dx = u_{i-1}^{(1)} a_1$$

$$\int_{I_{i+j}} q_1(x)dx = u_{i+j}^{(0)} a_0, \quad j=0,1; \qquad \int_{I_{i+1}} q_1(x) v_1^{(i+1)}(x)dx = u_{i+1}^{(1)} a_1$$

$$\int_{I_{i+j}} q_2(x)dx = u_{i+j}^{(0)} a_0, \quad j=-1,0,1$$

$$\int_{I_{i+j}} Q(x)dx = u_{i+j}^{(0)} a_0, \quad j=-1,0,1; \qquad \int_{I_{i+j}} Q(x) v_1^{(i+j)}(x)dx = u_{i+j}^{(1)} a_1, \quad j=-1,1.$$

Follow the routine A of WENO reconstruction, we can obtain new moment $u_i^{(1)}$.

Numerical Method

To reconstruct $u_i^{(2)}$:

$$\int_{I_{i+j}} q_0(x)dx = u_{i+j}^{(0)} a_0, \qquad \int_{I_{i+j}} q_0(x) v_1^{(i+j)}(x)dx = u_{i+j}^{(1)} a_1, \qquad j = -1, 0$$

$$\int_{I_{i+j}} q_1(x)dx = u_{i+j}^{(0)} a_0, \qquad \int_{I_{i+j}} q_1(x) v_1^{(i+j)}(x)dx = u_{i+j}^{(1)} a_1, \qquad j = 0, 1$$

$$\int_{I_{i+j}} q_2(x)dx = u_{i+j}^{(0)} a_0, \quad j = -1, 0, 1; \qquad \int_{I_i} q_2(x) v_1^{(i)} dx = u_i^{(1)} a_1$$

$$\int_{I_{i+j}} Q(x)dx = u_{i+j}^{(0)} a_0, \qquad \int_{I_{i+j}} Q(x) v_1^{(i+j)}(x)dx = u_{i+j}^{(1)} a_1, \qquad j = -1, 0, 1,$$

Follow the routine A of WENO reconstruction, we can obtain new moment $u_i^{(2)}$.

Remark III: For $\mathbb{P}^3$ case, we should extend stencil.

• New HWENO type reconstruction

I_i is a troubled cell, we use stencil $S = \{I_{i-1}, I_i, I_{i+1}\}$. Denote the solutions of the DG method on these three cells as polynomials $q_0(x)$, $q_1(x)$ and $q_2(x)$, respectively. We would like to modify $q_1(x)$ to $q_1^{new}(x)$.

Procedure by Zhong and Shu, JCP (2013):

In order to make sure that the reconstructed polynomial maintains the original cell average of q_1 in the target cell I_i, the following modifications are taken:

$$\tilde{q}_0 = q_0 - \overline{\overline{q}}_0 + \overline{\overline{q}}_1, \quad \tilde{q}_1 = q_1, \quad \tilde{q}_2 = q_0 - \overline{\overline{q}}_2 + \overline{\overline{q}}_1$$

$$\overline{\overline{q}}_0 = \frac{1}{\Delta x_i} \int_{I_i} q_0(x)dx, \quad \overline{\overline{q}}_1 = \frac{1}{\Delta x_i} \int_{I_i} q_1(x)dx, \quad \overline{\overline{q}}_2 = \frac{1}{\Delta x_i} \int_{I_i} q_2(x)dx,$$

Numerical Method

The final nonlinear WENO reconstruction polynomial $q_1^{new}(x)$ is now defined by a convex combination of these modified polynomials:

$$q_1^{new}(x) = \omega_0 \tilde{q}_0(x) + \omega_1 \tilde{q}_1(x) + \omega_2 \tilde{q}_2(x)$$

If $\omega_0 + \omega_1 + \omega_2 = 1$, then q_1^{new} has the same cell average and order of accuracy as q_1.

Computational formula of $\omega_0,\ \omega_1$, and ω_2 are same as in WENO reconstruction. The linear weights can be chosen to be any set of positive numbers adding up to one. Since for smooth solutions the central cell is usually the best one, a larger linear weight is put on the central cell than on the neighboring cells, i.e.

$$\gamma_0 < \gamma_1 \quad \text{and} \quad \gamma_1 > \gamma_2.$$

Numerical Method

In Zhong and Shu, JCP (2013), they take:

$$\gamma_0 = 0.001, \quad \gamma_1 = 0.998 \quad \gamma_2 = 0.001$$

which can maintain the original high order in smooth regions and can keep essentially non-oscillatory shock transitions in all their numerical examples.

Numerical Method

Procedure by Zhu, Zhong, Shu and Q. , 2013:

In order to make sure that the reconstructed polynomial maintains the original cell average of q_1 in the target cell I_i, the following modifications are taken:

$$\int_{I_{i-1}} (\tilde{q}_0(x) - q_0(x))^2 dx = \min \int_{I_{i-1}} (\phi(x) - q_0(x))^2 dx$$

$$\int_{I_{i+1}} (\tilde{q}_2(x) - q_2(x))^2 dx = \min \int_{I_{i+1}} (\phi(x) - q_2(x))^2 dx$$

for $\forall \phi(x) \in \mathbb{P}^k$ with $\int_{I_i} \phi(x)dx = \int_{I_i} q_1(x)dx$

For notational consistency we also denote $\tilde{q}_1(x) = q_1(x)$. Then we follow the routine of Zhong and Shu JCP (2013), and obtain the final nonlinear WENO reconstruction polynomial $q_1^{new}(x)$.

Numerical Method

For two dimensional case, we select the HWENO reconstruction stencil as $S = \{I_{i-1,j},\ I_{i,j-1},\ I_{i+1,j},\ I_{i,j+1},\ I_{ij}\}$ for simplify, we renumber these cells as I_ℓ, $\ell = 0, \cdots, 4$, and denote the DG solutions on these five cells to be $p_\ell(x,y)$, respectively.

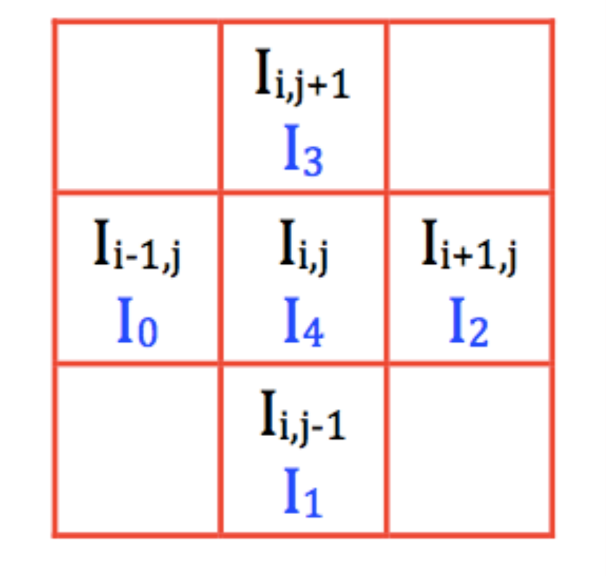

Numerical Method

$$\int_{I_\ell} (\tilde{p}_\ell(x,y) - p_\ell(x,y))^2 dxdy = \min \left\{ \int_{I_\ell} (\phi(x,y) - p_\ell(x,y))^2 dxdy \right.$$
$$\left. + \left(\int_{I_{\ell'}} (\phi(x,y) - p_{\ell'}(x,y)) dxdy \right)^2 + \left(\int_{I_{\ell''}} (\phi(x,y) - p_{\ell''}(x,y)) dxdy \right)^2 \right\},$$

for $\forall \phi(x,y) \in \mathbb{P}^k$ with $\int_{I_4} \phi(x,y)dxdy = \int_{I_4} p_4(x,y)dxdy$, where $\ell' = mod(\ell - 1, 4)$ and $\ell'' = mod(\ell + 1, 4)$.

For notational consistency we also denote $\tilde{p}_4(x,y) = p_4(x,y)$.

Then we follow the routine of WENO reconstruction:

- Take linear weights: $\gamma_0 = \gamma_1 = \gamma_2 = \gamma_3 = 0.001, \quad \gamma_4 = 0.996$

Numerical Method

- We compute the smoothness indicators,

$$\beta_\ell = \sum_{|\alpha|=1}^{k} |I_{ij}|^{|\alpha|-1} \int_{I_{ij}} \left(\frac{\partial^{|\alpha|}}{\partial x^{\alpha_1} \partial y^{\alpha_2}} \tilde{p}_\ell(x,y) \right)^2 dxdy, \ \ell = 0, \cdots, 4,$$

  where $\alpha = (\alpha_1, \alpha_2)$ and $|\alpha| = \alpha_1 + \alpha_2$.

- We compute the non-linear weights based on the smoothness indicators.

- The final nonlinear HWENO reconstruction polynomial $p_4^{new}(x,y)$ is defined by a convex combination of the (modified) polynomials in the stencil:

$$p_4^{new}(x,y) = \sum_{\ell=0}^{4} \omega_\ell \tilde{p}_\ell(x,y).$$

  $p_4^{new}(x,y)$ has the same cell average and order of accuracy as the original one $p_4(x,y)$ on condition that $\sum_{\ell=0}^{4} \omega_\ell = 1$.

3 Numerical results

We show the the numerical results of one- and two-dimensional cases to illustrate the performance of the WENO type limiters.

- Accuracy test
- Test cases with shock

Numerical results

Burgers equation $u_t + (u^2/2)_x = 0$. Initial condition $u(x,0) = 0.5 + \sin(\pi x)$ and periodic boundary condition. RKDG with a WENO limiter ($M = 0.01$) compared to RKDG without limiter. Lax–Friedrichs flux. $t = 0.5/\pi$. L_1 and L_∞ errors. Nonuniform meshes with N cells.

		DG with WENO limiter				DG with no limiter			
	N	L_1 error	Order	L_∞ error	Order	L_1 error	Order	L_∞ error	Order
P^1	10	4.61E-02		2.25E-01		1.39E-02		1.06E-01	
	20	1.16E-02	1.99	1.30E-01	0.79	3.53E-03	1.97	3.27E-02	1.70
	40	2.14E-03	2.44	2.53E-02	2.37	8.60E-04	2.04	9.10E-03	1.84
	80	2.85E-04	2.91	3.19E-03	2.99	2.11E-04	2.03	2.53E-03	1.85
	160	5.95E-05	2.26	7.42E-04	2.10	5.27E-05	2.00	6.73E-04	1.91
	320	1.45E-05	2.03	1.79E-04	2.05	1.31E-05	2.01	1.69E-04	1.99
P^2	10	5.98E-03		5.98E-02		1.95E-03		2.87E-02	
	20	5.52E-04	3.44	5.06E-03	3.56	2.72E-04	2.84	4.83E-03	2.57
	40	4.61E-05	3.58	8.97E-04	2.50	4.30E-05	2.66	8.39E-04	2.52
	80	6.22E-06	2.89	1.60E-04	2.48	6.23E-06	2.79	1.76E-04	2.26
	160	8.92E-07	2.80	2.55E-05	2.65	8.94E-07	2.80	2.52E-05	2.80
	320	1.28E-07	2.81	3.78E-06	2.75	1.27E-07	2.81	4.14E-06	2.60

Nonuniform Meshes

Numerical results

Burgers equation $u_t + (u^2/2)_x = 0$ with initial condition $u(x,0) = 0.5 + \sin(\pi x)$

N	DG with HWENO limiter				DG with no limiter			
	L_1 error	Order	L_∞ error	Order	L_1 error	Order	L_∞ error	Order
10	1.41E−02		8.09E−02		3.35E−03		2.21E−02	
20	1.12E−03	3.66	7.09E−03	3.51	4.00E−04	3.07	3.59E−03	2.62
40	7.99E−05	3.81	5.78E−04	3.62	5.11E−05	2.97	5.78E−04	2.64
80	8.34E−06	3.26	8.26E−05	2.81	6.46E−06	2.98	8.26E−05	2.81
160	9.97E−07	3.06	1.14E−05	2.86	8.14E−07	2.99	1.14E−05	2.86
320	1.22E−07	3.03	1.50E−06	2.92	1.02E−07	2.99	1.50E−06	2.92

DG3-HWENO5-RK3 and DG3-RK3 with no limiters. $t = 0.5/\pi$. L_1 and L_∞ errors. Uniform meshes with N cells.

Uniform Meshes

Nu

	cells	DG with HWENO limiter				DG without limiter			
	cells	L^1 error	order	L^∞ error	order	L^1 error	order	L^∞ error	order
P^1	10	4.24E-2		2.45E-1		1.38E-2		1.04E-1	
	20	7.96E-3	2.41	7.69E-2	1.67	3.52E-3	1.97	3.26E-2	1.67
	40	1.96E-3	2.01	1.64E-2	2.22	8.59E-4	2.03	9.11E-3	1.84
	80	2.62E-4	2.91	2.53E-3	2.69	2.11E-4	2.02	2.53E-3	1.85
	160	5.29E-5	2.30	6.73E-4	1.91	5.26E-5	2.00	6.72E-4	1.91
	320	1.31E-5	2.01	1.69E-4	1.99	1.31E-5	2.01	1.68E-4	1.99
P^2	10	1.73E-3		3.00E-2		1.72E-3		2.82E-2	
	20	2.02E-4	3.10	4.55E-3	2.72	2.01E-4	3.09	4.26E-3	2.73
	40	2.57E-5	2.97	7.26E-4	2.65	2.64E-5	2.93	6.71E-4	2.67
	80	3.21E-6	2.99	1.02E-4	2.83	3.28E-6	3.01	1.22E-4	2.45
	160	4.07E-7	2.98	1.38E-5	2.89	4.11E-7	2.99	1.51E-5	3.02
	320	5.19E-8	2.97	1.79E-6	2.94	5.24E-8	2.97	2.24E-6	2.75
P^3	10	2.93E-4		4.47E-3		1.76E-4		2.35E-3	
	20	1.88E-5	3.96	4.56E-4	3.29	1.66E-5	3.41	4.17E-4	2.50
	40	1.15E-6	4.02	3.64E-5	3.64	8.93E-7	4.22	3.67E-5	3.50
	80	7.33E-8	3.98	3.94E-6	3.21	5.40E-8	4.04	2.21E-6	4.05
	160	4.22E-9	4.11	2.91E-7	3.76	3.34E-9	4.01	1.43E-7	3.95
	320	2.08E-10	4.34	9.14E-9	4.99	2.08E-10	4.00	9.14E-9	3.97

Burgers' equation, New HWENO limiter, Uniform Meshes

Numerical results

Euler equations. Initial condition $\rho(x,y,0) = 1 + 0.2\sin(\pi(x+y))$, $u(x,y,0) = 0.7$, $v(x,y,0) = 0.3$, $p(x,y,0) = 1$ and periodic boundary conditions. RKDG with WENO limiter ($M = 0.01$) compared to RKDG without limiter. Lax–Friedrichs flux. $t = 2.0$. L_1 and L_∞ errors for the density ρ. Nonuniform meshes with $N \times N$ cells.

		DG with WENO limiter				DG with no limiter			
	$N \times N$	L_1 error	Order	L_∞ error	Order	L_1 error	Order	L_∞ error	Order
P^1	10×10	3.48E-02		7.34E-02		1.11E-02		3.15E-02	
	20×20	6.89E-03	2.34	2.74E-02	1.42	1.91E-03	2.55	1.04E-02	1.60
	40×40	1.21E-03	2.51	7.36E-03	1.89	3.70E-04	2.37	2.93E-03	1.83
	80×80	2.33E-04	2.37	2.02E-03	1.87	8.15E-05	2.18	7.82E-04	1.91
	160×160	5.19E-05	2.17	6.45E-04	1.65	1.93E-05	2.08	2.04E-04	1.94
P^2	10×10	1.26E-03		8.22E-03		5.95E-04		8.89E-03	
	20×20	9.97E-05	3.66	1.21E-03	2.76	6.88E-05	3.11	1.18E-03	2.91
	40×40	9.61E-06	3.38	1.50E-04	3.02	8.41E-06	3.03	1.50E-04	2.98
	80×80	1.10E-06	3.12	1.90E-05	2.98	1.04E-06	3.01	1.90E-05	2.98
	160×160	1.34E-07	3.04	2.40E-06	2.98	1.30E-07	3.00	2.40E-06	2.98

Nonuniform Meshes

Numerical results

WENO limiter on unstructured meshes

2D-Euler equations: initial data $\rho(x,y,0) = 1 + 0.2\sin(\pi(x+y))$, $u(x,y,0) = 0.7$, $v(x,y,0) = 0.3$, and $p(x,y,0) = 1$

	h	DG with WENO limiter				DG without limiter			
		L^1 error	Order	L^∞ error	Order	L^1 error	Order	L^∞ error	Order
P^1	2/10	3.76E − 2		8.37E − 2		4.39E − 3		2.23E − 2	
	2/20	1.16E − 2	1.69	3.50E − 2	1.26	1.03E − 3	2.08	5.42E − 3	2.04
	2/40	2.36E − 3	2.31	1.25E − 2	1.48	2.54E − 4	2.02	1.29E − 3	2.06
	2/80	3.99E − 4	2.56	3.83E − 3	1.70	6.38E − 5	1.99	3.27E − 4	1.98
	2/160	7.33E − 5	2.44	1.16E − 3	1.72	1.62E − 5	1.97	8.48E − 5	1.95
P^2	2/10	4.01E − 3		1.76E − 2		4.48E − 4		5.94E − 3	
	2/20	6.50E − 4	2.63	3.47E − 3	2.34	6.17E − 5	2.86	1.14E − 3	2.38
	2/40	8.37E − 5	2.96	4.94E − 4	2.81	7.05E − 6	3.12	1.94E − 4	2.56
	2/80	1.01E − 5	3.04	6.60E − 5	2.91	7.76E − 7	3.18	2.87E − 5	2.76
	2/160	1.26E − 6	3.01	7.09E − 6	3.21	1.10E − 7	2.81	3.62E − 6	2.99

Periodic boundary conditions in both directions. $t = 2.0$. L^1 and L^∞ errors. RKDG with the WENO limiter ($M = 0.01$) compared to RKDG without limiter. The mesh points on the boundary are uniformly distributed with cell length h.

Numerical results

2D Euler equation, HWENO limiter

$N \times N$	DG with HWENO limiter				DG with no limiter			
	L_1 error	Order	L_∞ error	Order	L_1 error	Order	L_∞ error	Order
10×10	7.15E−03		5.26E−02		7.94E−04		5.53E−03	
20×20	2.67E−04	4.75	1.10E−03	5.59	1.03E−04	2.95	8.79E−04	2.65
40×40	2.66E−05	3.32	1.29E−04	3.08	1.26E−05	3.03	1.28E−04	2.78
80×80	2.36E−06	3.49	1.71E−05	2.92	1.50E−06	3.07	1.71E−05	2.91
160×160	2.19E−07	3.43	2.17E−06	2.97	1.81E−07	3.05	2.17E−06	2.97

unstructured meshes

		DG with HWENO limiter				DG without limiter			
	h	L^1 error	order	L^∞ error	order	L^1 error	order	L^∞ error	order
P^2	2/10	2.30E-3		1.33E-2		4.48E-4		5.94E-3	
	2/20	3.29E-4	2.81	1.69E-3	2.98	6.17E-5	2.86	1.14E-3	2.38
	2/40	4.45E-5	2.89	2.78E-4	2.60	7.05E-6	3.12	1.94E-4	2.56
	2/80	5.51E-6	3.01	4.17E-5	2.74	7.76E-7	3.18	2.87E-5	2.76
	2/160	6.95E-7	2.99	5.17E-6	3.00	1.10E-7	2.81	3.62E-6	2.99

Numerical results

厦门大学 Xiamen University

2D Euler quation, New HWENO limiter

		DG with HWENO limiter				DG without limiter			
	cells	L^1 error	order	L^∞ error	order	L^1 error	order	L^∞ error	order
P^1	10×10	3.29E-2		5.90E-2		2.55E-2		4.44E-2	
	20×20	4.25E-3	2.95	1.23E-2	2.26	3.72E-3	2.78	7.71E-3	2.52
	40×40	6.09E-4	2.80	2.77E-3	2.15	5.29E-4	2.81	1.51E-3	2.35
	80×80	1.03E-4	2.56	5.67E-4	2.29	9.14E-5	2.53	4.73E-4	1.67
	160×160	2.00E-5	2.37	1.43E-4	1.99	1.89E-5	2.27	1.30E-4	1.86
P^2	10×10	8.02E-4		6.16E-3		7.95E-4		5.52E-3	
	20×20	1.02E-4	2.97	8.84E-4	2.80	1.02E-4	2.95	8.78E-4	2.65
	40×40	1.37E-5	2.90	1.26E-4	2.80	1.25E-5	3.03	1.28E-4	2.77
	80×80	1.55E-6	3.14	1.70E-5	2.89	1.49E-6	3.07	1.70E-5	2.91
	160×160	1.81E-7	3.10	2.17E-6	2.97	1.81E-7	3.04	2.17E-6	2.97
P^3	10×10	1.50E-4		6.45E-4		4.86E-5		6.70E-4	
	20×20	2.85E-6	5.72	4.04E-5	4.00	2.85E-6	4.08	4.04E-5	4.05
	40×40	1.75E-7	4.03	2.49E-6	4.02	1.75E-7	4.03	2.49E-6	4.02
	80×80	1.08E-8	4.01	1.55E-7	4.01	1.08E-8	4.02	1.55E-7	4.01
	160×160	6.76E-10	4.00	9.71E-9	3.99	6.75E-10	4.00	9.68E-9	4.00

厦门大学 Xiamen University

Numerical results

Average and maximum percentages of cells flagged as troubled cells subject to different troubled-cell indicators for the Lax problem, and the quality of the solutions.

N	Schemes indicator	P^1			P^2			P^3		
		Ave	Max	Osc	Ave	Max	Osc	Ave	Max	Osc
200	TVB-1	10.68	22.00		12.70	24.00		16.31	29.00	
	TVB-2	1.87	4.50		2.56	5.50		3.87	5.50	L
	BDF	8.75	17.00		21.52	39.00		19.53	33.00	
	BSB	8.22	17.00		20.73	36.00		21.62	33.00	
	MP	28.61	36.50		27.95	41.00		32.54	41.50	
	MMP	13.24	22.00	Y	11.05	22.50	L	11.97	21.50	L
	KXRCF	1.33	3.00	L	2.10	3.50		2.46	4.50	
	Harten	3.85	9.00	L	1.00	5.00	L	2.07	6.50	L
400	TVB-1	8.55	17.50		11.02	21.75		13.66	26.00	
	TVB-2	1.37	2.75		1.82	3.50		3.29	4.50	
	BDF	7.86	15.75		19.29	36.75		17.09	34.00	
	BSB	6.57	12.50		18.96	35.50		16.23	24.75	
	MP	16.94	25.50		17.71	28.25		18.94	26.00	
	MMP	9.87	19.00	Y	9.06	18.25	L	9.23	17.00	L
	KXRCF	0.98	1.75	L	1.36	2.75		1.70	3.25	
	Harten	2.51	6.00		0.59	2.75		1.47	6.00	

Lax problem: Euler equations with initial condition

$$(\rho, v, p) = \begin{cases} (0.445, 0.698, 3.528) & \text{if } x \le 0, \\ (0.5, 0, 0.571) & \text{if } x > 0. \end{cases}$$

Numerical results

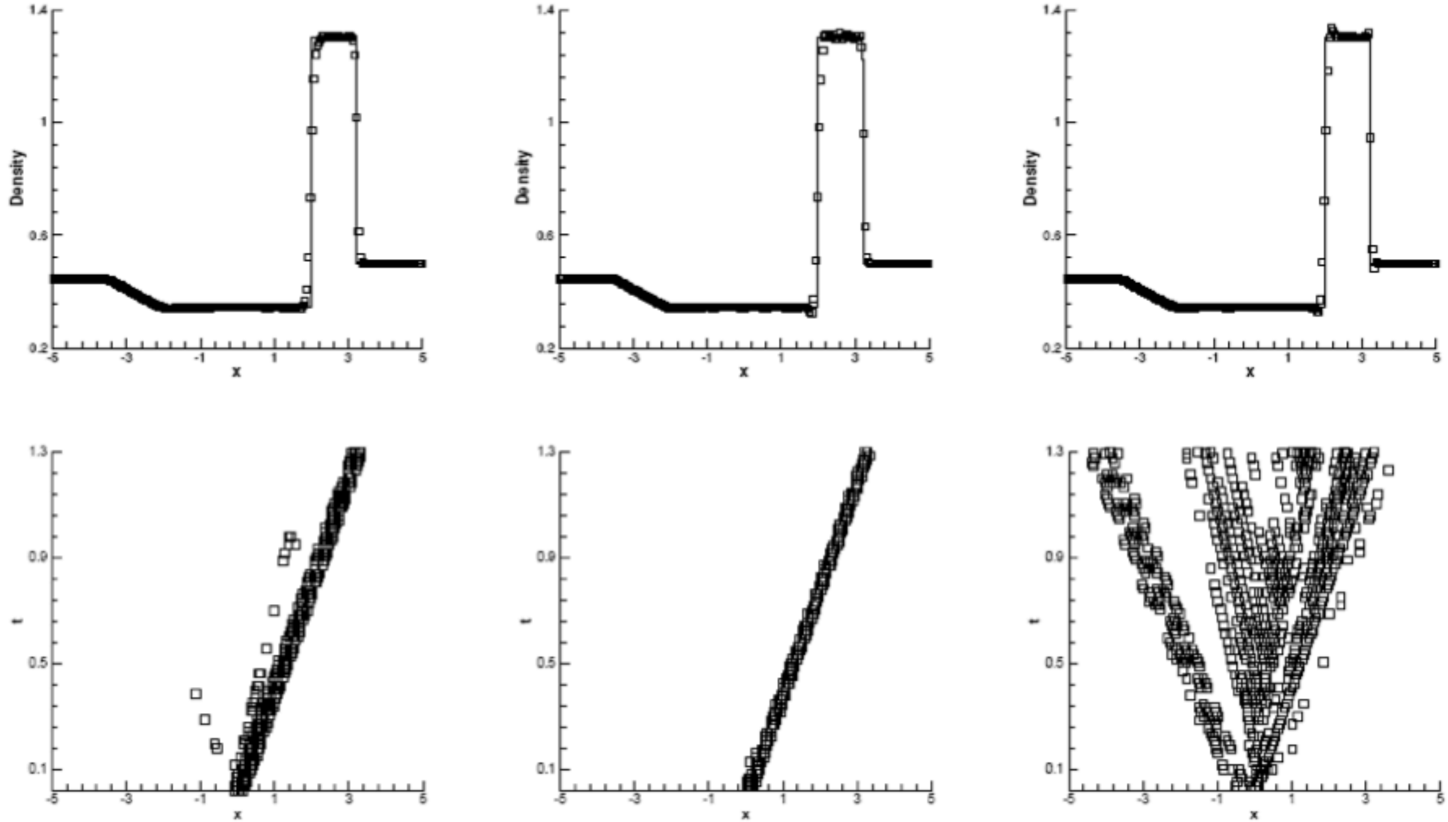

K=1 TVB(M=10) indicator KXRCF indicator Harten indicator

Nu

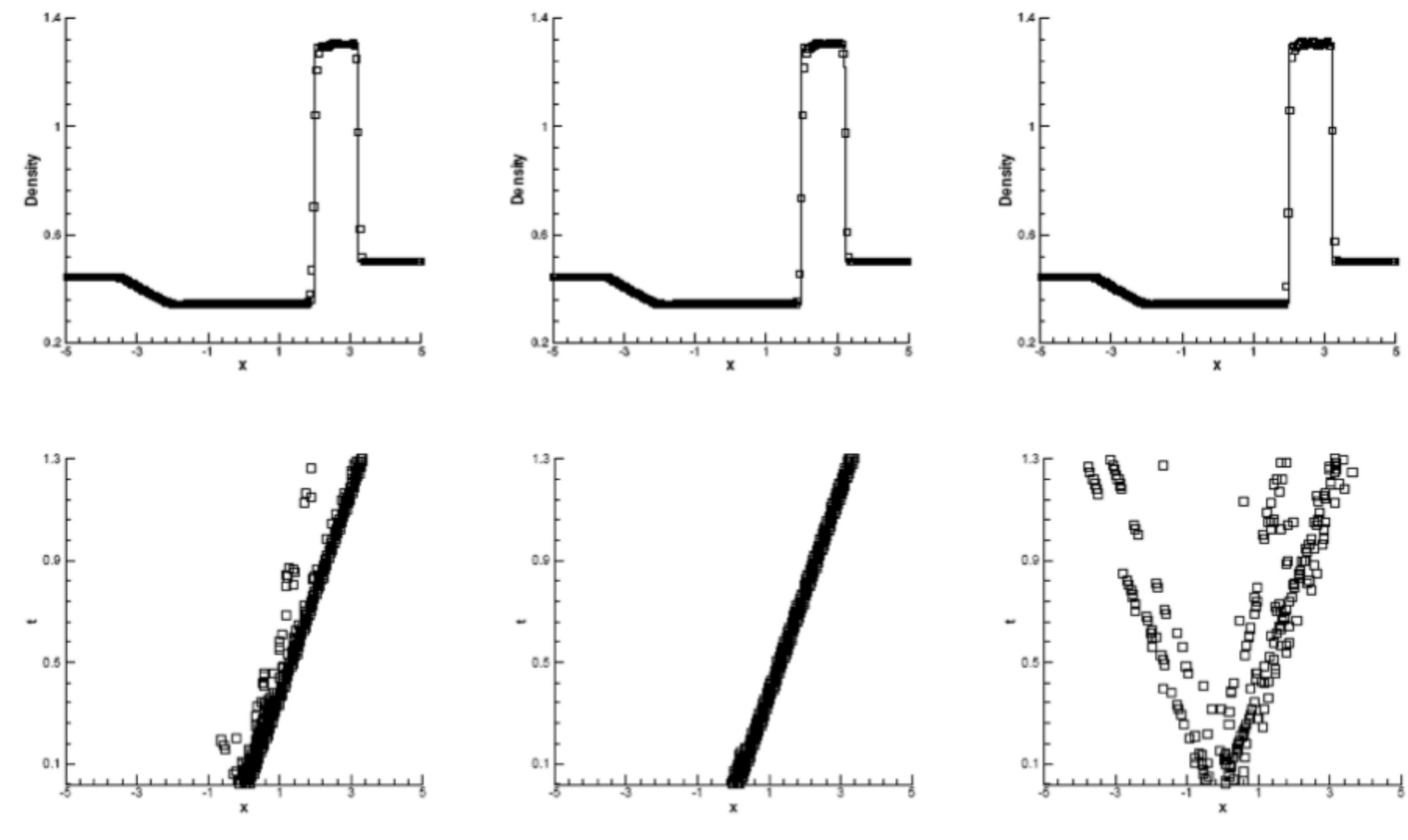

K=2 TVB (M=10) indicator KXRCF indicator Harten indicator

Nu

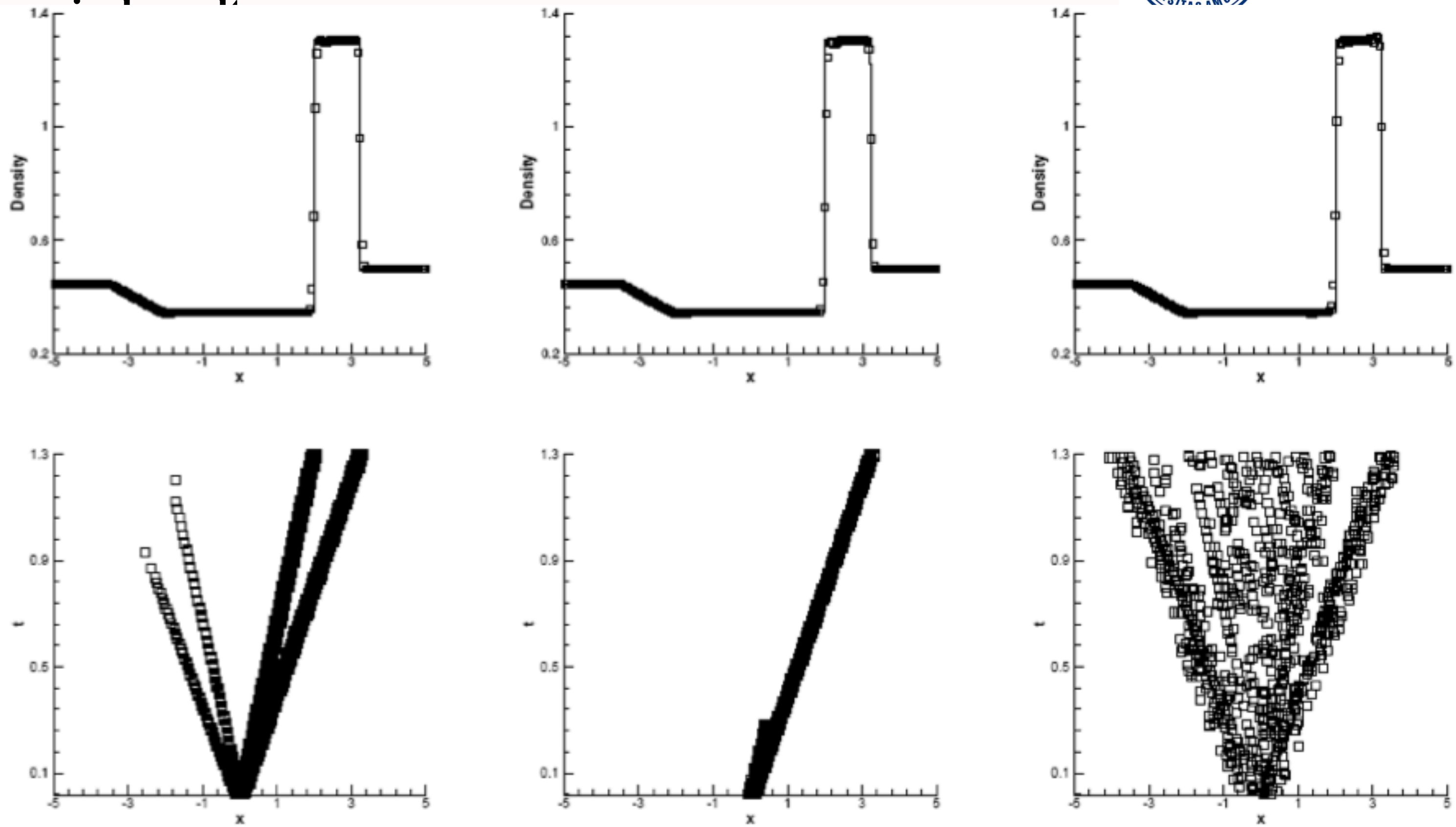

K=3 TVB-2(M=10) indicator KXRCF indicator Harten indicator

Nu

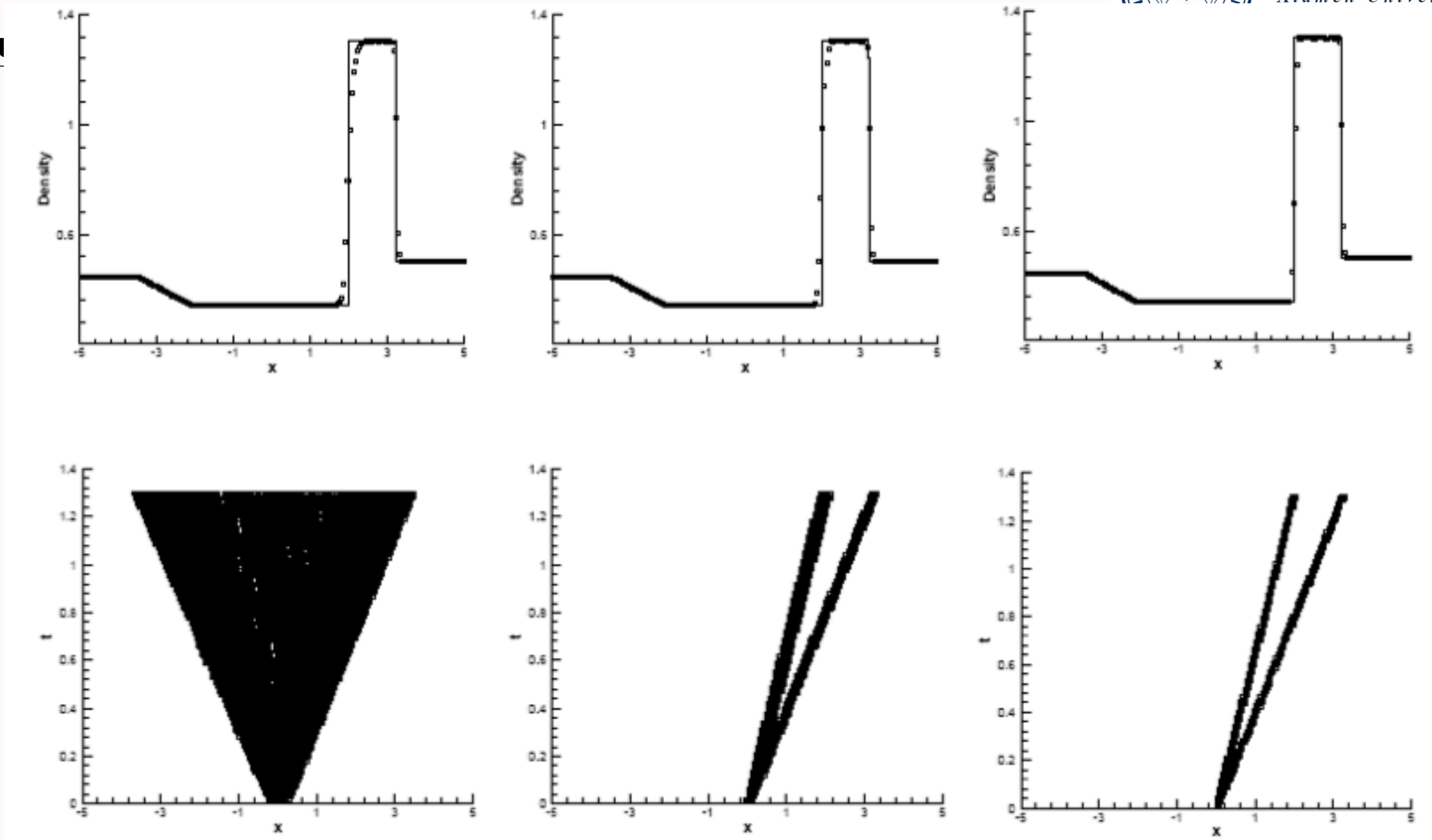

Lax problem. HWENO limiter, K=2,
TVB constant M=0.01,10,50

Nu

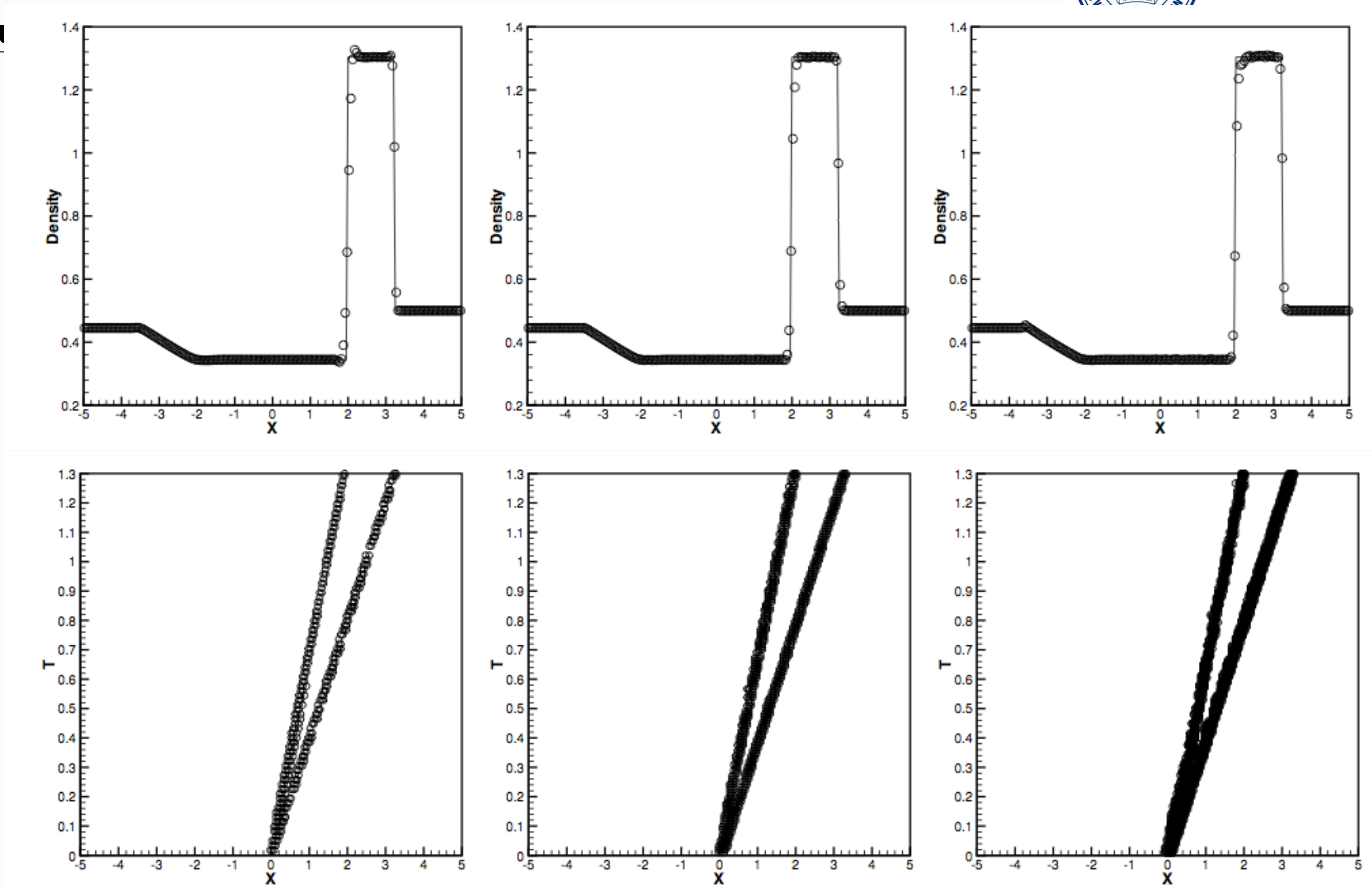

New HWENO limiter, P^1, P^2 and P^3 from left to right using KXRCF troubled-cell indicator.

Numer

Average and maximum percentages of cells flagged as troubled cells subject to different troubled-cell indicators for the blast wave problem, and the quality of the solutions.

N	Schemes indicator	P^1			P^2			P^3		
		Ave	Max	Osc	Ave	Max	Osc	Ave	Max	Osc
200	TVB-1	16.56	27.00		15.83	28.50		19.10	34.00	
	TVB-3	9.50	19.50		10.90	19.00		13.87	24.00	
	BDF	15.21	26.50		40.83	63.00		48.70	71.00	
	BSB	13.95	23.00		34.43	48.50		50.33	72.00	
	MP	22.90	38.50		21.89	41.50		24.35	41.50	
	MMP	12.98	22.50		11.46	22.00		12.76	23.50	
	KXRCF	13.66	23.50		15.29	22.50		20.17	29.00	
	Harten	3.59	9.50		1.67	7.00		3.66	11.00	
400	TVB-1	11.07	19.50		11.47	24.25		13.53	26.00	
	TVB-3	6.90	11.75		8.30	15.25		10.04	17.25	
	BDF	10.24	20.25		35.10	51.75		43.08	69.25	
	BSB	9.88	15.50		28.30	41.25		41.74	61.50	
	MP	14.22	25.25		15.41	26.75		17.87	31.75	
	MMP	8.69	14.00		9.08	16.50	L	8.68	18.25	L
	KXRCF	8.45	14.00		10.16	13.75		14.24	20.50	
	Harten	2.11	5.50		0.97	3.50		3.03	8.75	

Blast wave problem: Euler equations with initial condition

$$(\rho, v, p) = \begin{cases} (1, 0, 1000) & \text{if } 0 \le x < 0.1, \\ (1, 0, 0.01) & \text{if } 0.1 \le x < 0.9, \\ (1, 0, 100) & \text{if } 0.9 \le x \le 1. \end{cases}$$

Numerical results

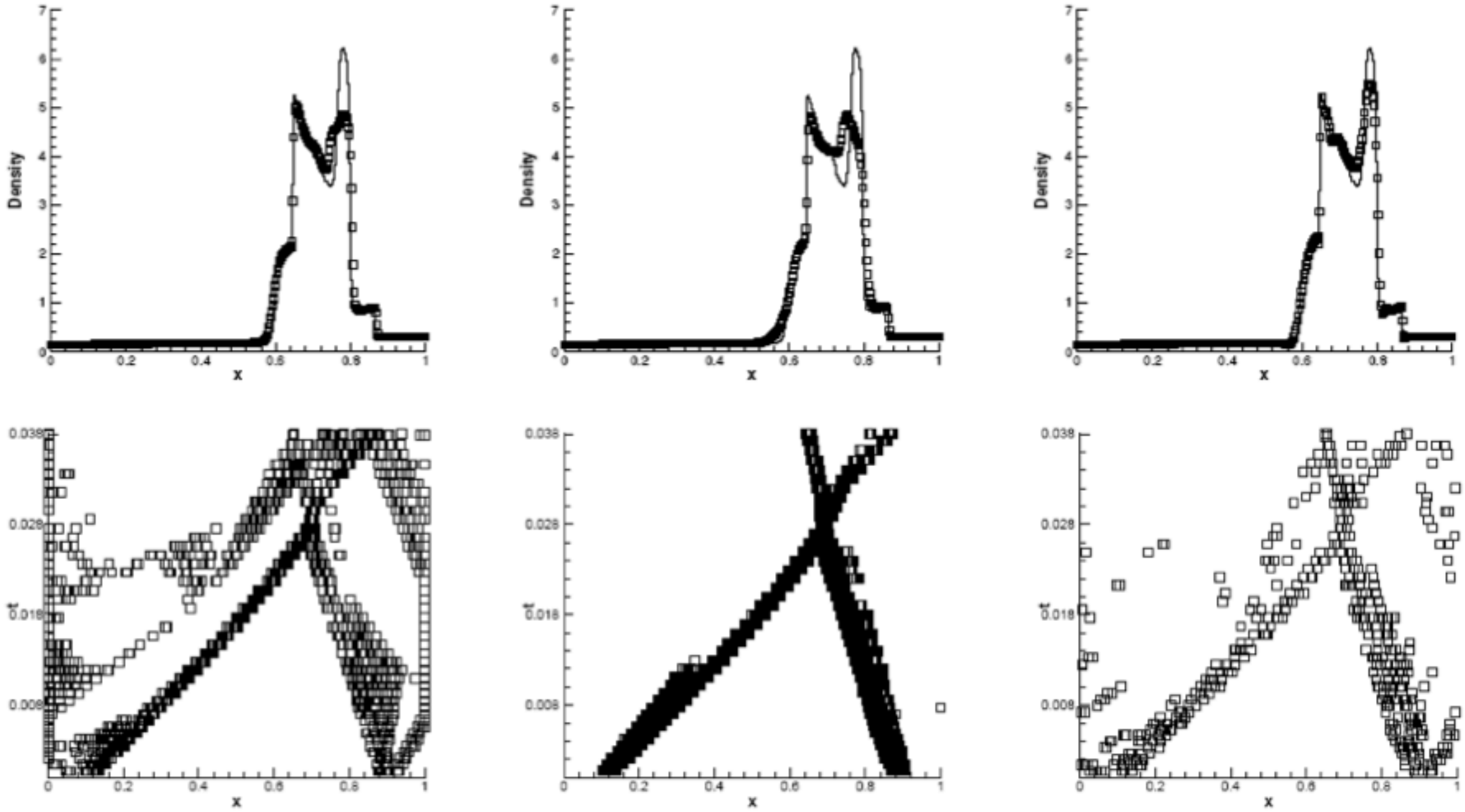

K=1 TVB (M=100.) indicator KXRCF indicator Harten indicator

Nu

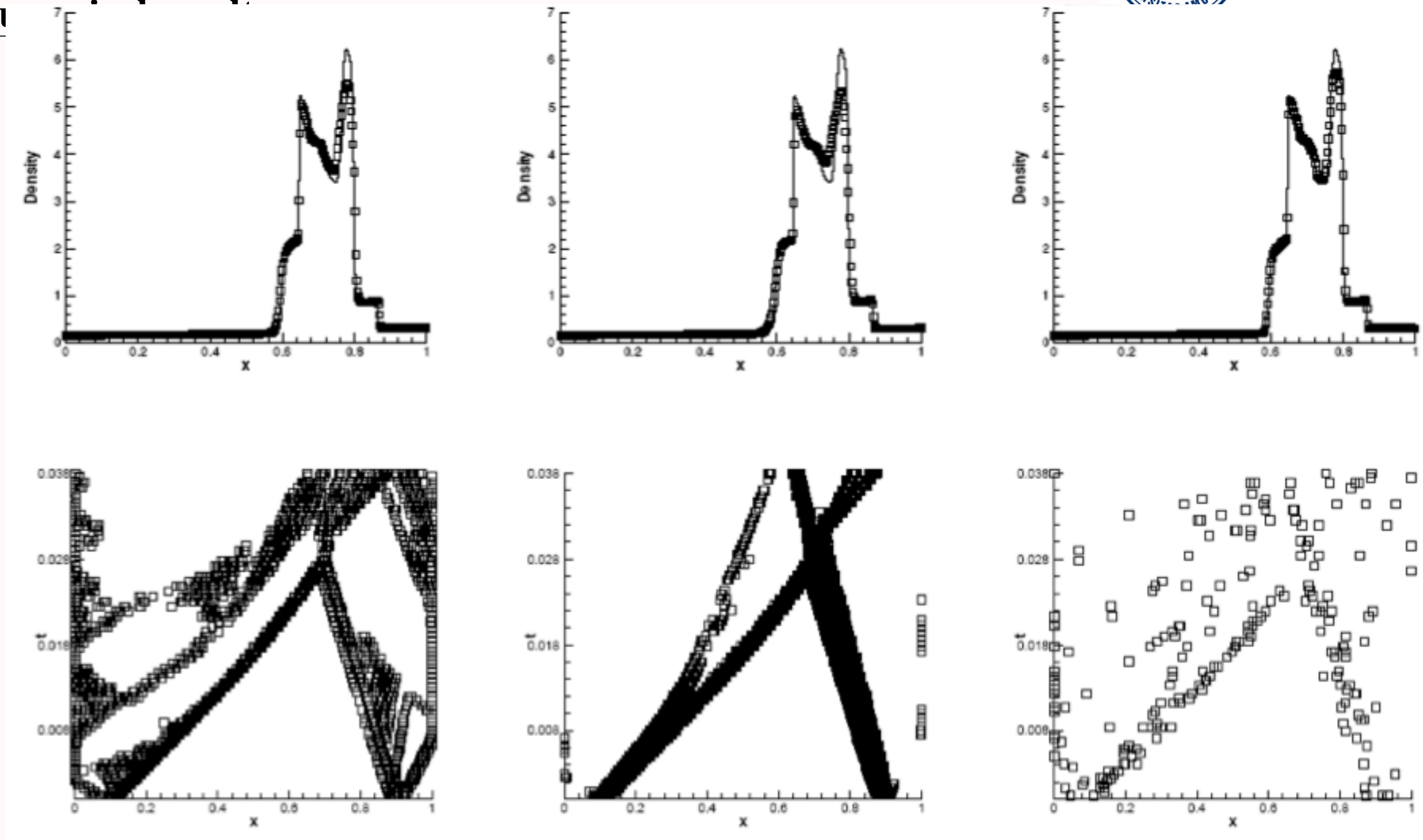

K=2 TVB (M=100.) indicator KXRCF indicator Harten indicator

Nu

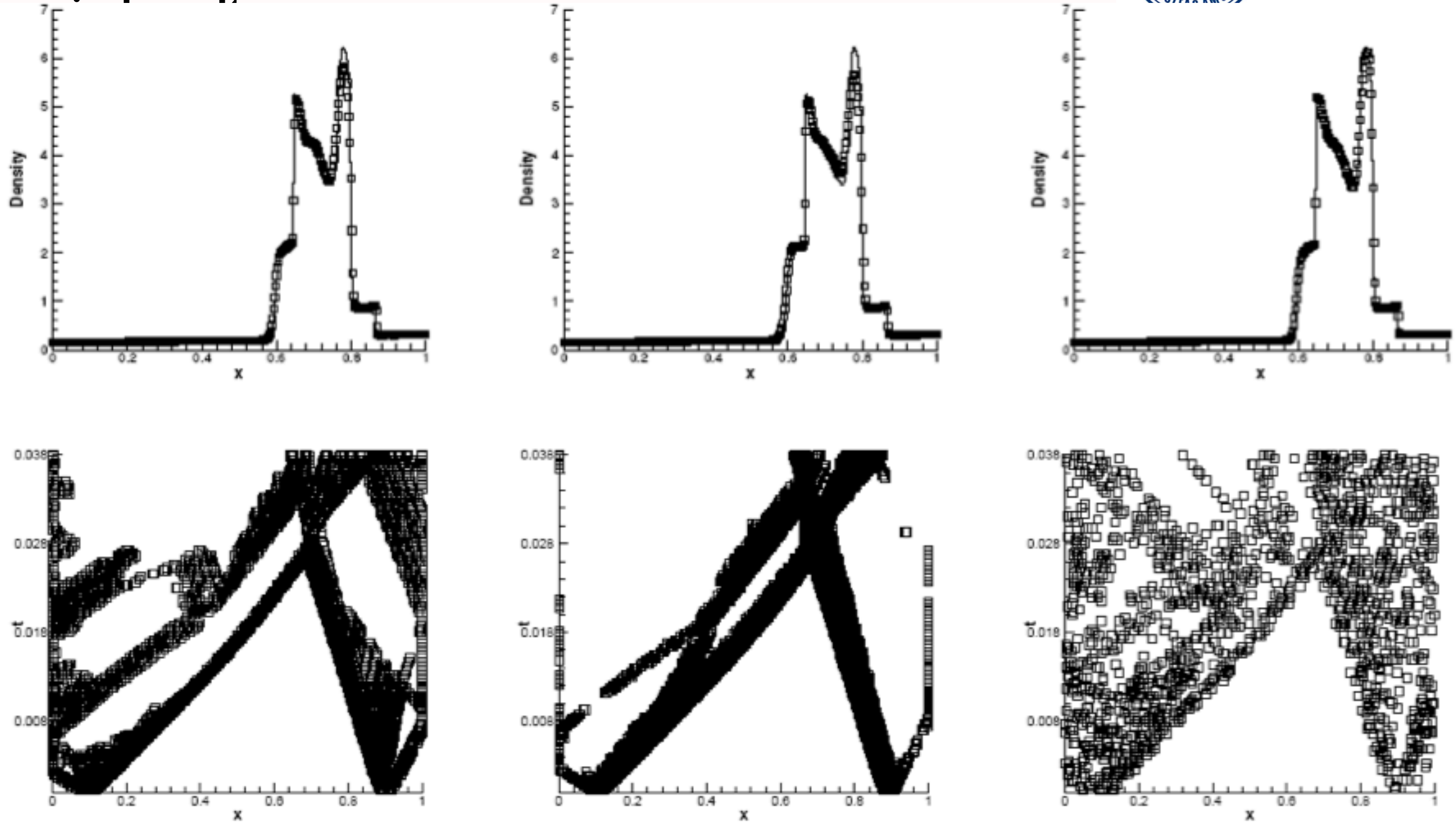

K=3 TVB (M=100.) indicator KXRCF indicator Harten indicator

Nu

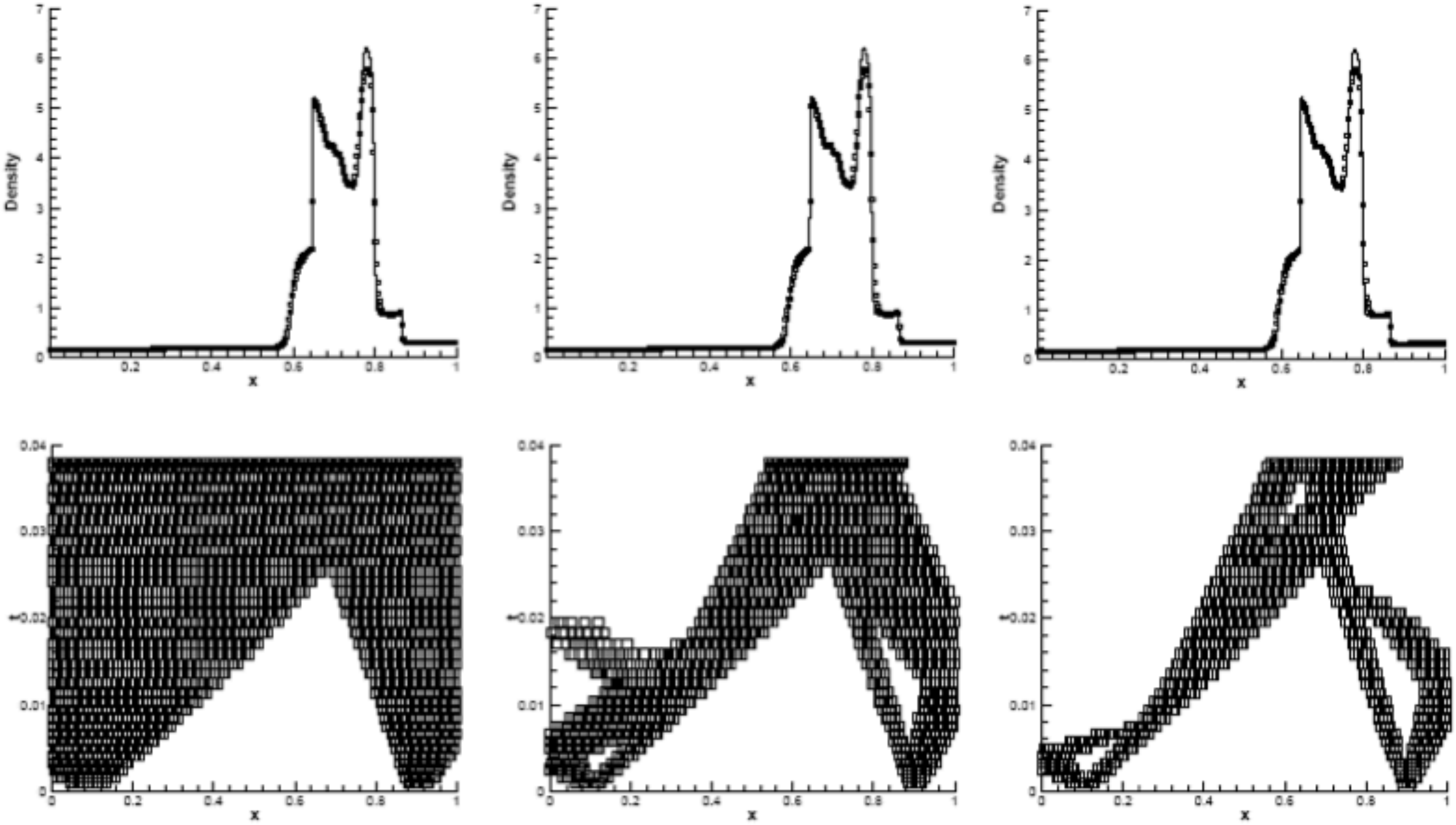

The blast wave problem. HWENO limiter, K=2, TVB constant M=0.01,50,300.

Nu

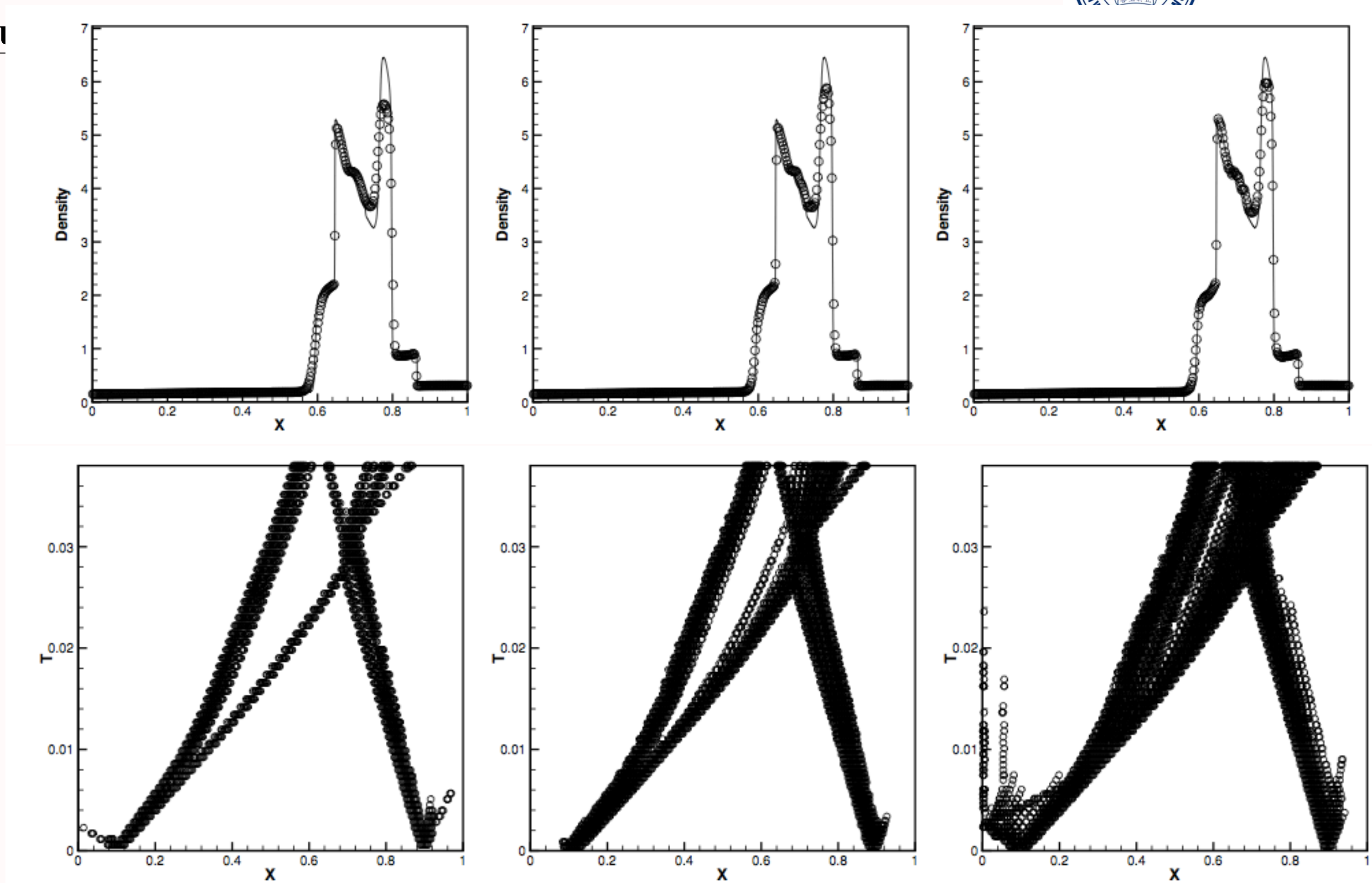

New HWENO limiter, P^1, P^2 and P^3 from left to right using KXRCF troubled-cell indicator.

- Two-dimensional Euler equations

The PDEs are

$$\begin{pmatrix} \rho \\ \rho u \\ \rho v \\ E \end{pmatrix}_t + \begin{pmatrix} \rho u \\ \rho u^2 + p \\ \rho u v \\ u(E+p) \end{pmatrix}_x + \begin{pmatrix} \rho v \\ \rho u v \\ \rho v^2 + p \\ v(E+p) \end{pmatrix}_y = 0.$$

- Double mach reflection problem

The computational domain for this problem is $[0, 4] \times [0, 1]$. The reflecting wall lies at the bottom, starting from $x = \frac{1}{6}$. Initially a right-moving Mach 10 shock is positioned at $x = \frac{1}{6}$, $y = 0$ and makes a 60° angle with the x-axis. For the bottom boundary, the exact post-shock condition is imposed for the part from $x = 0$ to $x = \frac{1}{6}$ and a reflective boundary condition is used for the rest. At the top boundary, the flow values are set to describe the exact motion of a Mach 10 shock. We compute the solution up to $t = 0.2$.

Numerical results

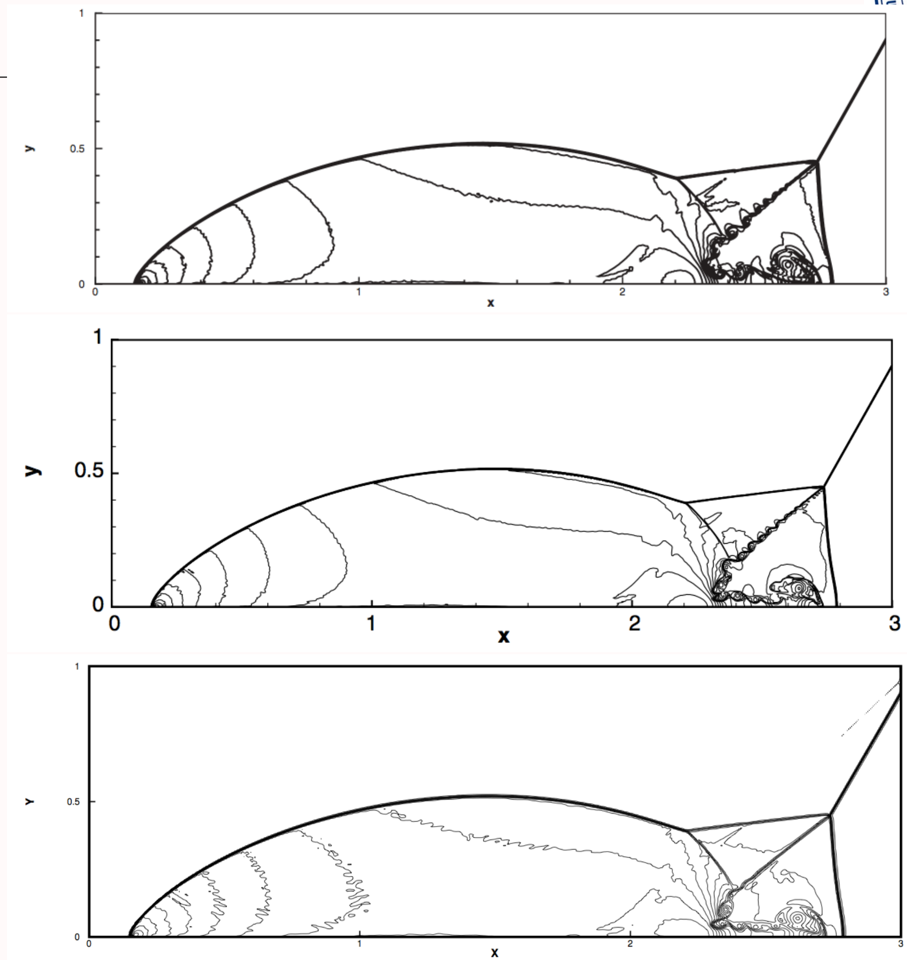

Form top to bottom, WENO limiter (1920×480 cells), HWENO limiter (1920×480 cells) and New HWENO limiter (800×200 cells).

- **Forward step problem**

A Mach 3 wind tunnel with a step. The wind tunnel is 1 length unit wide and 3 length units long. The step is 0.2 length units high and is located 0.6 length units from the left-hand end of the tunnel. The problem is initialized by a right-going Mach 3 flow. Reflective boundary conditions are applied along the wall of the tunnel and in/out flow boundary conditions are applied at the entrance/exit. We compute the solution up to $t = 4$.

Numerical results

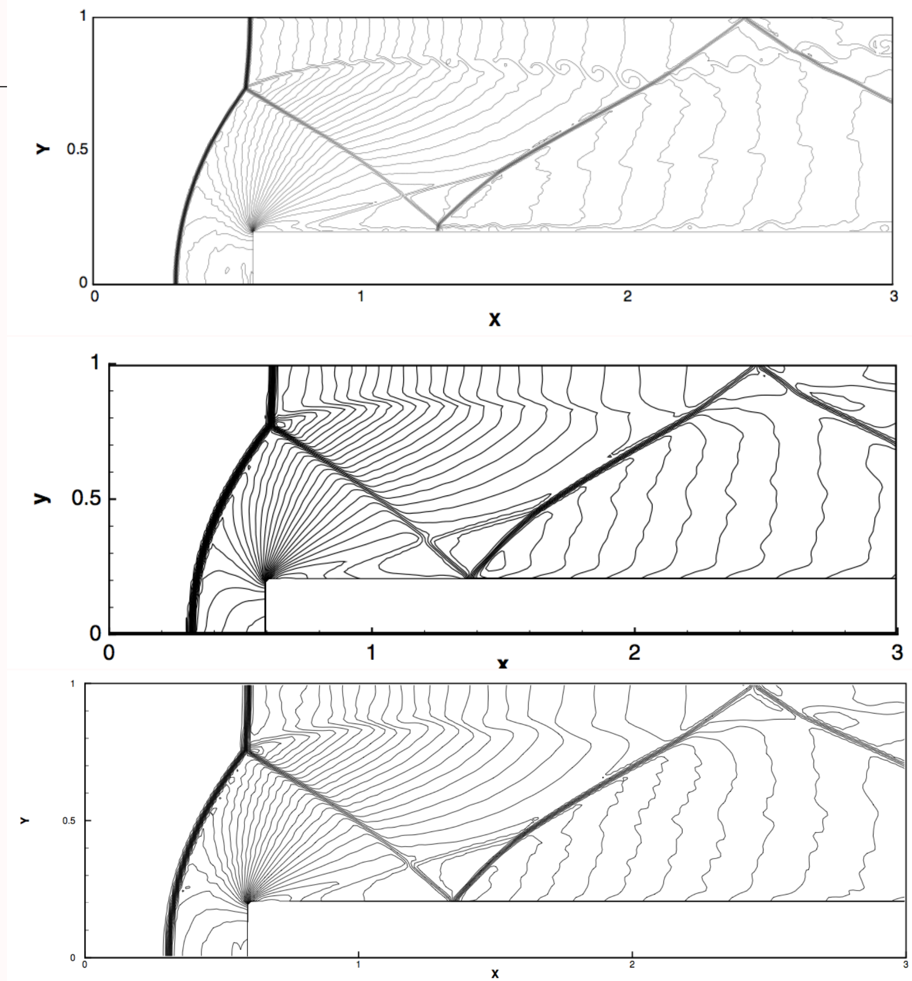

Form top to bottom, WENO limiter (480 × 160 cells), HWENO limiter (240 × 80 cells) and New HWENO limiter (240 × 80 cells).

4 Adaptive methods with different indicators

- h-method: mesh refinement
- p-method: order enrichment
- r-method: mesh motion (moving mesh method)

What is the connection between the adaptive methods and the troubled-cell indicators?

- For the h-method, the key point is to identify where the mesh should be refined and coarsened.
- Troubled cell indicators tell us where the discontinuities are.
- We can refine the troubled cells and coarsen cells which are not troubled.

Adaptive methods with different indicators

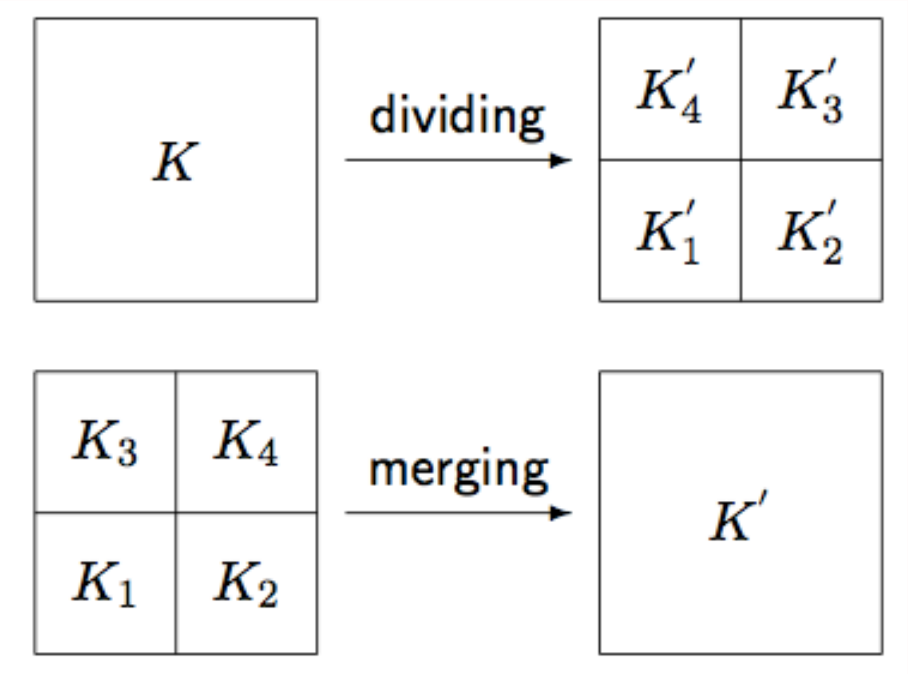

Sketches of and dividing (top) and merging (bottom) in the adaptive mesh

Adaptive methods with different indicators

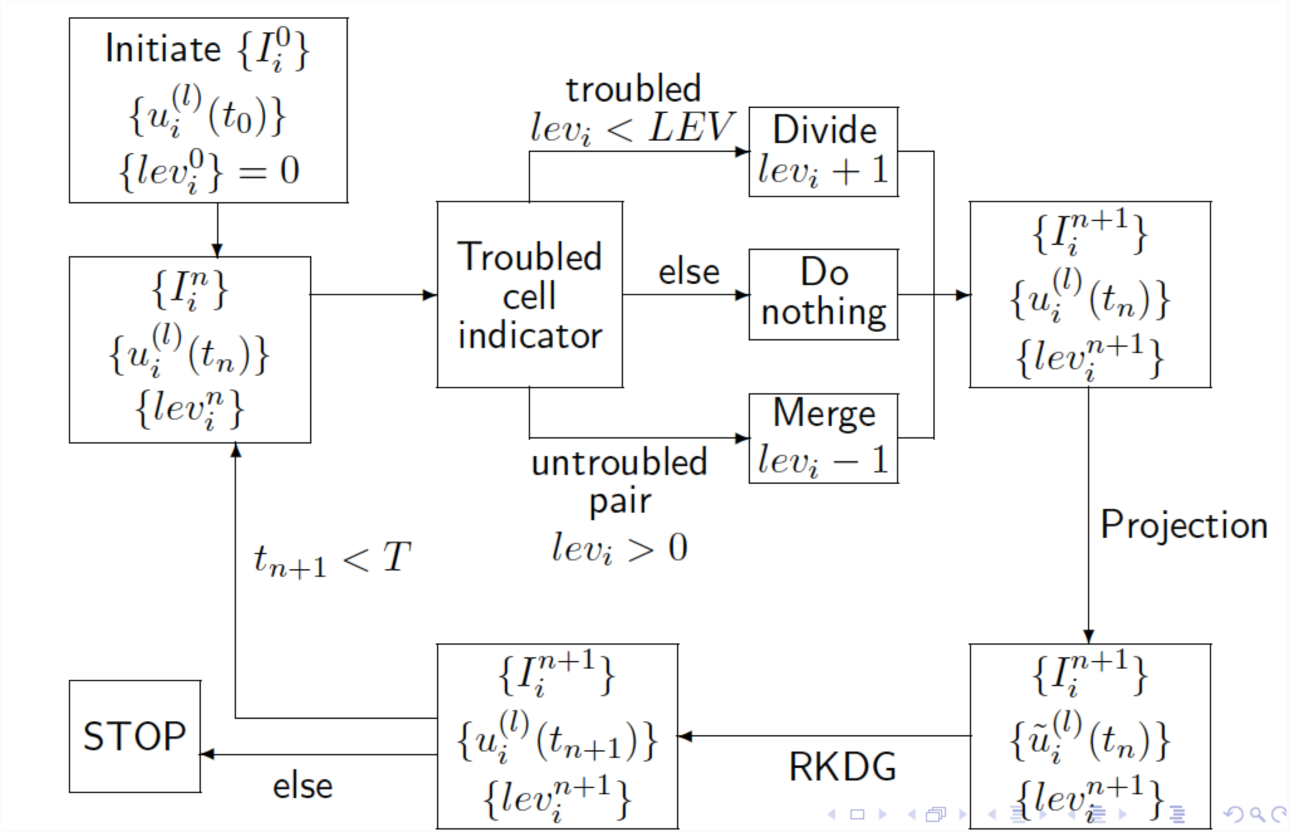

Algorithm of h-method using troubled cell indicators

5 Hybrid WENO with different indicators

- Drawback of WENO schemes
  - The computation of the nonlinear weights is costly.
  - Local characteristic decomposition is need necessarily to avoid spurious oscillations for the system case.
  - The drawback is more evident with the increase of the space dimension and the number of equation.

Hybrid WENO with different indicators

- In order to overcome the drawback
  - We investigate hybrid schemes of WENO schemes with high order up-wind linear schemes using different discontinuity indicators to explore the possibility in avoiding the local characteristic decompositions and the nonlinear weights for part of the procedure.
  - The main idea is to identify discontinuity by a discontinuity indicator, then to reconstruct numerical flux by WENO approximation at discontinuity and by up-wind linear approximation at smoothness.
  - These indicators are mainly based on the troubled-cell indicators for DG methods.

Hybrid WENO with different indicators

- Solving nonlinear hyperbolic conservation laws

$$u_t + f(u)_x = 0.$$

- A semidiscrete conservative scheme

$$\frac{du_j(t)}{dt} = -\frac{1}{\Delta x}(\hat{f}_{j+1/2} - \hat{f}_{j-1/2}),$$

  where $\hat{f}_{j+1/2}$ is the numerical flux.

- For stability purpose, the flux is split into two parts, such as by Lax-Friedrichs splitting:

$$f^{\pm} = \frac{1}{2}(f(u) \pm \alpha u).$$

  Then we take $\hat{f}_{j+1/2} = \hat{f}^+_{j+1/2} + \hat{f}^-_{j+1/2}$. $\hat{f}^+_{j+1/2}$ and $\hat{f}^-_{j+1/2}$ are relative to $f^+(u)$ and $f^-(u)$, respectively.

Hybrid WENO with different indicators

Step 1. The troubled-cell indicator is applied to identify troubled cell only once at the beginning of the Runge-Kutta time discretization procedure.

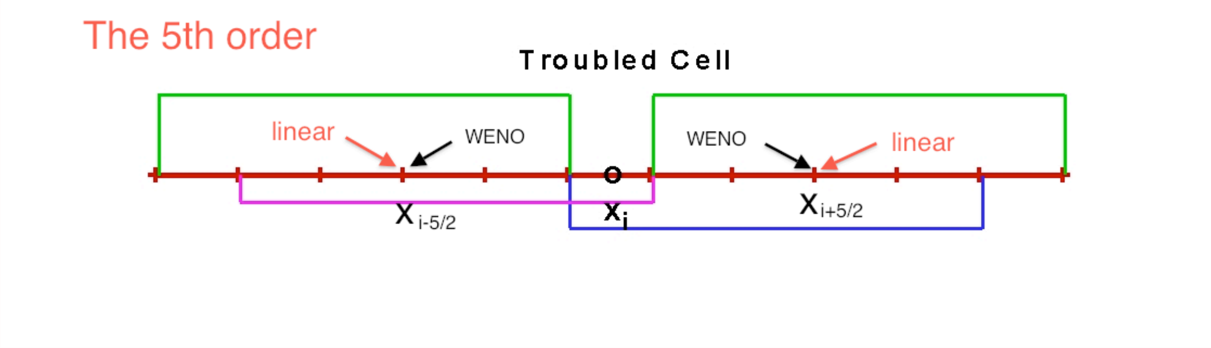

Step 2.

- To reconstruct the numerical flux based on the $2r+1$ order WENO approximation in the discontinuous vicinage.

- Otherwise, by the $2r+1$ order up-wind linear approximation in the smooth vicinage.

Hybrid WENO with different indicators

The procedure for the reconstruction of numerical flux $\hat{f}^+_{j+1/2}$ by WENO approximation and high order up-wind linear approximation.

- WENO approximation

$$\hat{f}^+_{j+1/2} = \sum_{k=0}^{r} \omega_k q_k^r(f^+_{j+k-r}, \dots, f^+_{j+k}), \tag{1}$$

here ω_k is the nonlinear weight, and

$$q_k^r(\mathrm{g}_0, \dots, \mathrm{g}_r) = \sum_{l=0}^{r} a^r_{k,l}\mathrm{g}_l \tag{2}$$

are the low order approximation to $\hat{f}^+_{j+1/2}$ on the kth stencil $S_k = (x_{j+k-r}, \dots, x_{j+k}), k = 0, 1, \dots, r$.

Hybrid WENO with different indicators

- The smoothness indicator

$$IS_k = \sum_{l=1}^{r} \int_{x_{j-1/2}}^{x_{j+1/2}} (\Delta x)^{2l-1} (q_k^{(l)})^2 dx,$$

where $q_k^{(l)}$ is the lth-derivative of $q_k(x)$ and $q_k(x)$ is the reconstruction polynomial of $f^+(u)$ on stencil S_k such that

$$\frac{1}{\Delta x} \int_{I_i} q_k(x) dx = f_i^+, \; i = j+k-r, \ldots, j+k.$$

Hybrid WENO with different indicators

- The nonlinear weight

We compute the nonlinear weight ω_k based on the smoothness indicator

$$\omega_k = \frac{\alpha_k}{\sum_{l=0}^{r} \alpha_l}, \text{ with } \alpha_k = \frac{C_k^r}{(\varepsilon + IS_k)^2}, \; k = 0, 1, \ldots, r,$$

where C_k^r is the *linear weights*.

Hybrid WENO with different indicators

- Up-wind linear approximation

We use all the r candidate stencils, i.e., $S = \bigcup_{k=0}^{r} S_k$, to obtain a 2r+1 order approximation to $\hat{f}^+_{j+1/2}$ in smooth parts such that:

$$\frac{1}{\Delta x}\int_{I_i} q_r^{2r+1}(x)dx = f_i^+,\ i = j-r,\dots,j+r,$$

and

$$\hat{f}^+_{j+1/2} = q_r^{2r+1}(f^+_{j-r},\dots,f^+_{j+r}) = \sum_{l=0}^{2r} b_l f^+_{j+l-r}.$$

- The formulas for the negative part of the flux $\hat{f}^-_{j+1/2}$ are mirror symmetric with respect to $x_{j+1/2}$.

- Remark of the two kinds of approximations
  - For the system cases, the WENO approximation is always performed with a local characteristic decomposition.
  - While the up-wind linear approximation is performed component by component.
  - For two dimensional cases, the reconstruction of fluxes is based on dimension by dimension.

Hybrid WENO with different indicators

- Comparison between WENO approximation and up-wind linear approximation
  - The cost of computation of nonlinear weights is very expensive due to the smoothness indicators. So the WENO approximation is more costly than the up-wind linear approximation.
  - In the smooth parts of the solution, both the two approximation can result in the same high order accuracy.
  - However, the WENO approximation is crucial when the strong discontinuities such as shock wave is present. The only usage of up-wind linear approximation would generate spurious numerical oscillations.

Hybrid WENO with different indicators

Double Mach reflection problem. Comparison on CPU time and percentage of reconstruction of fluxes by WENO approximation.

$N_x \times N_y$	Scheme or indicators	3rd-order scheme		5th-order scheme	
		CPU	Percent	CPU	Percent
960×240	WENO	5928.03	100.00	9374.70	100.00
	ATV	1145.37	6.99	1433.27	7.44
	TVB-3	1050.23	3.55	1379.08	5.96
	MR	1064.82	5.38	1256.15	5.78
	KXRCF	1312.24	3.61	1505.23	4.39
1920×480	WENO	40262.41	100.00	62511.25	100.00
	ATV	10530.14	5.61	11384.43	6.03
	TVB-3	8150.48	2.72	11048.70	5.29
	MR	7759.46	3.56	9536.02	3.88
	KXRCF	8817.95	2.30	11257.59	3.24

6 Conclusions

- We have developed a new limiter for the RKDG methods solving hyperbolic conservation laws using finite volume high order WENO and HWENO reconstructions.
- First identify troubled cells by troubled cell indicator.
- Then reconstruct the polynomial solution inside the troubled cells by WENO type reconstruction using the cell averages and moments of neighboring cells, while maintaining the original cell averages of the troubled cells.
- Systematically studied and compared a few different procedures to identify troubled cells.

Conclusions

- Numerical results show that the method is stable, accurate and robust in maintaining accuracy.
- Troubled cell indicator was used as discontinuous indicator for h-adaptive and r-adaptive methods and hybrid WENO methods.

Refereces

1. J. Qiu and C.-W. Shu: J. Comput. Phys., 193 (2004) 115-135.
2. J. Qiu and C.-W. Shu: Computers & Fluids , 34 (2005) 642-663.
3. J. Qiu and C.-W. Shu: SIAM J. Sci. Comput., 26 (2005), 907-929.
4. J. Qiu and C.-W. Shu: SIAM J. Sci. Comput., 27 (2005), 995-1013.
5. J. Zhu, J. Qiu, C.-W. Shu and M. Dumbser: J. Comput. Phys., 227 (2008) 4330-4353.
6. J. Zhu and J. Qiu: J. Sci. Comput., 39 (2009), 293-321.
7. H. Zhu and J. Qiu: J. Comput. Phys., 228 (2009) , 6957-6976.
8. G. Li and J. Qiu: J. Comput. Phys., 229 (2010), 8105-8129.
9. J. Zhu and J. Qiu: J. Comput. Phys., 230 (2011), 4353-4375.
10. J. Zhu and J. Qiu: Commun.Comput. Phys., 11 (2012), 985-1005.
11. G. Li, C. Lu and J. Qiu: J. Sci. Comput., 51 (2012), 527-559.
12. J. Zhu and J. Qiu: J. Sci. Comput., 55 (2013), 606-644.
13. H. Zhu, Y. Cheng and J. Qiu: Adv. Appl. Math. Mech., 5 (2013), 365-390.
14. J. Zhu, X. Zhong, C.-W. Shu and J. Qiu: J. Comput. Phys., 248 (2013), 200-220.
15. H. Zhu and J. Qiu: Adv. Comput. Math., 39(2013), 445-463.
16. G. Li and J. Qiu: Adv. Comput. Math., to appear
17. J. Zhu, X. Zhong, C.-W. Shu and J. Qiu: *Runge-Kutta discontinuous Galerkin method with a simple and compact Hermite WENO limiter*, preprint.

THANK YOU!

jxqiu@xmu.edu.cn
http://ccam.xmu.edu.cn/teacher/jxqiu